haematologica
Journal of the Ferrata Storti Foundation

Therapeutic inhibition of myeloperoxidase with AZD5904 attenuates disease progression in mouse models of early-stage and relapsed multiple myeloma

by Connor M.D. Williams, Jacqueline E. Noll, Dylan Harnas, Hayley B. Parkinson, Duncan R. Hewett, Andrew C.W. Zannettino, Kate Vandyke, Thomas R. Cox and Vasilios Panagopoulos

Received: December 15, 2025.
Accepted: March 16, 2026.

Citation: Connor M.D. Williams, Jacqueline E. Noll, Dylan Harnas, Hayley B. Parkinson, Duncan R. Hewett, Andrew C.W. Zannettino, Kate Vandyke, Thomas R. Cox and Vasilios Panagopoulos. Therapeutic inhibition of myeloperoxidase with AZD5904 attenuates disease progression in mouse models of early-stage and relapsed multiple myeloma.
Haematologica. 2026 Apr 2. doi: 10.3324/haematol.2025.300383 [Epub ahead of print]

Therapeutic inhibition of myeloperoxidase with AZD5904 attenuates disease progression in mouse models of early-stage and relapsed multiple myeloma

Connor M.D. Williams [1,2], Jacqueline E. Noll [1,2], Dylan Harnas [1,2], Hayley B. Parkinson [1,2], Duncan R Hewett [1,2], Andrew C.W. Zannettino [1,2], Kate Vandyke [1,2], Thomas R. Cox [3,4 *], and Vasilios Panagopoulos [1,2,5*]

**Contributed equally.*

Corresponding Author: bill.panagopoulos@adelaide.edu.au

1. Myeloma Research Laboratory, School of Pharmacy and Biomedical Science, College of Health, Adelaide University, Adelaide, Australia
2. Precision Cancer Medicine Theme, The South Australian Health and Medical Research Institute, Adelaide, Australia
3. The Garvan Institute of Medical Research & the Kinghorn Cancer Centre, Translational Oncology Program, Sydney, NSW, Australia
4. School of Clinical Medicine, St Vincent's Healthcare Clinical Campus, Faculty of Medicine and Health, UNSW Sydney, Sydney, NSW, Australia
5. Centre for Cancer Biology, Adelaide University, Adelaide, SA, Australia

Running head: Targeting MPO to control MM relapse

Funding: This project was supported by grant 2021451 and awarded through the 2022 Priority-driven Collaborative Cancer Research Scheme and co-funded by Cancer Australia, Can Too Foundation and Leukaemia Foundation. JN was supported by a Cancer Council South Australia Mid-Career Fellowship. TRC was supported by the National Health and Medical Research Council (2033065). VP was supported by a National Health and Medical Research Council Early Career Fellowship.

Disclosures: The authors have no conflicts of interests to disclose.

Acknowledgements: The authors thank AstraZeneca for providing AZD5904 for these studies through the Open Innovation Program.

Data Sharing Statement: The data that support the findings of this study are available from the corresponding author upon reasonable request

Contributions: Conceptualisation by VP and TC. Methodology and design by CW, JN, DH, BP, TC. Investigation by CW, JN, HP, DH. Writing (original draft) preparation by CW, JN, TC, VP. Writing (review and editing) by CW, JN, KV, AZ, TC, VP. Supervision by JN, KV, AZ, VP. Final approval of manuscript by all authors.

Abstract:

Despite advances in therapeutic strategies for multiple myeloma (MM), long-term outcomes remain poor, largely due to inevitable relapse and acquired drug resistance. Reciprocal interactions between malignant MM plasma cells (PCs) and the bone marrow microenvironment (BMME) drive disease progression, immune evasion, and therapeutic resistance, positioning the BM niche as a focus for targeted therapeutics. Myeloperoxidase (MPO) has recently emerged as a key regulator of MM progression via modification of the BMME. Here, we evaluate the efficacy of AZD5904, an orally bioavailable, irreversible MPO inhibitor, in preclinical models of MM. Initiation of MPO inhibition with AZD5904 during the early stages of MM tumour development significantly reduced tumour burden in the KaLwRij/5TGM1 and Vk*Myc murine models, however had no effect when initiated in established disease. Furthermore, AZD5904 modulated immune responses by decreasing $PD1^+$ T cells *in vivo* and restoring $CD8^+$ T cell cytotoxicity *in vitro*. While combining AZD5904 with the frontline agent bortezomib did not provide additional benefit in limiting disease progression, adjuvant AZD5904 following bortezomib treatment markedly delayed 5TGM1 tumour relapse. These findings suggest that while MPO inhibition may not enhance efficacy of bortezomib induction therapy, it holds promise as a maintenance strategy to improve long-term outcomes in MM. Collectively, our data support further investigation of AZD5904 as a novel maintenance therapy targeting the BM microenvironment, with potential to enhance and sustain the effectiveness of existing, standard of care regimens.

Introduction:

Multiple myeloma (MM) is a haematological malignancy characterised by the clonal expansion of abnormal plasma cells (PCs) within the bone marrow (BM). Despite significant advancements in therapies contributing to improved outcomes for MM patients, the median survival still remains limited to only 6 to 8 years post diagnosis.[1] One of the most challenging aspects in the clinical management of MM is the inevitable and recurrent relapse following induction therapy.[2,3] Acquired therapeutic resistance and subsequent relapse, coupled with a growing understanding of the bone marrow microenvironment (BMME) as a crucial driver of MM progression, highlights the need for a more comprehensive approach to treatment strategies that not only target active disease, but also strengthen induction and/or maintenance therapies to prolong relapse free survival.

The accumulation of the inflammatory enzyme myeloperoxidase (MPO) within the tumour microenvironment has emerged as a potential regulator of tumour development in some solid cancers, primarily due to its potent pro-oxidative and pro-inflammatory properties.[4,5] Additionally, myeloid derived suppressor cells (MDSC), a heterogenous population of immature myeloid cells with potent immunosuppressive capabilities, have emerged as a prominent source of MPO in cancer.[6] Importantly, MDSC are known to accumulate in the PB and BM of MM patients and are recognized as major contributors to poor patient outcomes due to their immunosuppressive activity**.**[7-10] We have previously reported a functional role for MPO in driving MM progression. Specifically, we demonstrated that pharmacological inhibition of MPO using 4-aminobenzoic acid hydrazide (4-ABAH) impeded MM tumour progression *in vivo*.[11] Notably, AZD5904 has emerged as a potent, orally bioavailable, irreversible, 2-thioxantine inhibitor of MPO, which covalently attaches to the heme group of the enzyme, inhibiting enzymatic activity and impairing ROS formation**.**[12] Unlike 4-ABAH, AZD5904 has passed phase I clinical trials and shown efficacy in modulating chronic obstructive pulmonary disease.[13]

The present study assessed the use of AZD5904 as a novel therapeutic agent for the management of MM, both as a monotherapy, as well as in combination with the MM induction therapy mainstay agent, bortezomib. We confirm that MPO protein is increased in MM tumour bearing mice, with circulating levels of MPO correlating with disease stage *in vivo*. Importantly, we show that AZD5904 monotherapy is efficacious in impeding MM disease progression when treatment is initiated at early stages of disease. Whilst combination approaches with bortezomib yielded no additional benefit compared to bortezomib alone, we demonstrate that, when used as a maintenance therapy following bortezomib induction therapy, AZD5904 is effective in significantly delaying relapse in a murine model of MM. Collectively, these findings support the further investigation of MPO inhibition with AZD5904 as a potential maintenance therapeutic strategy, to be explored alongside current standard of care treatments.

Methods

Animal Ethics

The use of animals was approved by the South Australian Health and Medical Research Institute (SAHMRI) Animal Ethics Committee (SAM-20-022, SAM-22-007).

KaLwRij/5TGM1 transplant model

Six-to-eight-week old male C57BL/KaLwRij were inoculated with $5x10^5$ luciferase expressing 5TGM1 cells in 100 µl PBS via the tail vein (i.v.) as previously described.[14] Tumour progression was quantified by bioluminescent imaging (BLI) using the Xenogen IVIS® Spectrum Imaging System.

Vk*MYC transplant model

Eight-week-old C57BL/6J mice were inoculated with Vk14451-GFP whole BM, originally provided by Dr Michelle McDonald (Garvan Institute, NSW, Australia). Mice were injected i.v. with $2.5x10^4$ MM PCs in 100 µl PBS. MM tumour development was monitored over 10 weeks by weekly serum paraprotein electrophoresis (SPEP) as previously described.[15]

AZD5904 and bortezomib administration (*in vivo*)

Where indicated, AZD5904 (AstraZeneca) was administered via oral gavage (p.o.), twice daily at 150 mg/kg/day in 100 µl 0.5% hydroxypropyl methylcellulose, 0.1% TWEEN80 in sterile MilliQ. Bortezomib (SelleckChem) was injected i.v twice weekly at a dose of 0.2 mg/kg or 1 mg/kg as indicated, in 3% DMSO/PBS.

Flow cytometric analysis

For analysis of myeloid populations, total BM was isolated from long bones and stained with CD11b APC-Cy7 (BD Biosciences, 561039), Ly-6C BV421, and Ly-6G PE-Cy7 antibodies (Biolegend, 128031 and 127617). For analysis of T cell populations, RBC depleted splenocytes and complete BM were stained with CD4 PECy7 (Biolegend, 100421), CD8a APC-Cy7, and PD1 PE (BD Biosciences, 561967 and 568261) antibodies. Samples were analysed on an LSRFortessa X-20 flow cytometer. Data was analysed using FlowJoTM Software v10.6 (BD).

$CD8^+$ cytotoxicity assays

C57BL/KaLwRij $CD8^+$ T cells (Supplementary Methods) were cocultured with or without native human MPO (hMPO; 2 µg/mL) and AZD5904 (20 µM, 100 µM) in the presence of gamma-irradiated (30 Gy) 5TGM1 cells at 10:1 effector:target ratio for 72 hrs. T cells were harvested and re-seeded in a 96-well plate at $3x10^4$ cells/well with $1x10^4$ irradiated-5TGM1 cells in 1% FCS T cell medium

and cultured for 24 hours. Cytotoxicity was determined using a lactate dehydrogenase (LDH) assay kit (Promega Corporation) as per manufacturer's instructions.

In vitro bortezomib cytotoxicity assays

For monoculture assays, 5TGM1 MM PCs were seeded at a density of $2x10^4$ cells/well with 2 µg/mL hMPO (Cell Sciences Inc.) in a 96-well plate. After 24 hours, bortezomib (1 nM, 2.5 nM, 5 nM, 10 nM) or vehicle control (0.02% DMSO) was added. After a further 24 hours, the relative number of 5TGM1 cells per well was quantified using luminescent imaging as previously described.[16]

For coculture assays, KaLwRij BM mesenchymal stromal cells (BM-MSCs) (Supplementary Methods), were seeded at $2.5x10^4$ cells/cm^2 in triplicate in a 96 well black walled flat bottom plate and allowed to adhere overnight. Media was aspirated the following day prior to the addition of 2 µg/mL hMPO (Cell Sciences Inc.) in α-MEM media. After 24 hours, 5TGM1 MM PCs were added at a density of $2x10^4$ cells/well in 20% FCS Iscove's Modified Dulbecco's Medium (IMDM). Cells were allowed to adhere for 1 or 8 hour/s prior to the addition of varying concentrations of bortezomib (1 nM, 2.5 nM, 5 nM, 10 nM). After 24 hours, the relative number of 5TGM1 cells per well was quantified using luminescent imaging, as previously described.[16]

Results

MPO is increased in myeloma tumour-bearing mice

Building on clinical reports of increased $CD11b^+$ myeloid cells in early-diagnosed and relapsed MM patients[17], we previously demonstrated that $CD11b^+$ cells are enriched within the BM of 5TGM1 tumour-bearing mice and exhibit increased *Mpo* mRNA expression.[11] To further investigate the significance of increased Mpo expression in the BM microenvironment driven by MM tumour development *in vivo*, we measured levels of circulating Mpo in MM tumour bearing mice at early and late stages of disease progression. We found a significant increase in the concentration of circulating Mpo at late stages of disease (6720 pg/ml) compared to that seen in naïve C57BL/KaLwRij mice (2778 pg/mL) (p=0.0007; Figure 1Ai-ii), which correlated with BM tumour burden (Figure 1Aiii). Furthermore, consistent with our previous findings, we confirmed that $CD11b^+$ myeloid cells are enriched in the BM of an alternative murine model of MM. Vk*Myc tumour bearing C57BL/6J mice exhibit a 1.4-fold increase in $Cd11b^+$ myeloid cells within the BM after 9 weeks of tumour development (Figure 1Bi), which is accompanied by an upregulation in *Mpo* mRNA expression (Figure 1Bii). Furthermore, increased *Mpo* expression by myeloid cells within the BM was strongly correlated with BM tumour burden (Figure 1Biii). Similar to our observations in 5TGM1 tumour bearing C57BL/KaLwRij mice, this upregulation in *Mpo* expression in late stage disease coincides with a significant increase in circulating levels of Mpo with Vk*Myc tumour development (17 583 pg/mL) compared to naïve controls (12 540 pg/mL) (p=0.0158; Figure 1Biv).

Targeted inhibition of MPO using AZD5904 delays MM progression.

We have previously demonstrated that inactivation of MPO with 4-ABAH is a viable therapeutic strategy in a mouse model of MM.[11] Here, we aimed to replicate these findings using AZD5904, a potent, orally bioavailable, irreversible inhibitor of myeloperoxidase (MPO) that has been evaluated in Phase I clinical trials for the treatment of chronic inflammatory diseases.[18] In line with our previous findings, systemic inhibition of MPO with AZD5904 in both the KaLwRij/5TGM1 and Vk*Myc mouse models significantly reduced tumour burden when compared to mice receiving a vehicle control, when treatment was initiated 24 hr prior to tumour cell inoculation. Specifically, 5TGM1 tumour burden was reduced by 49.26%, as determined by BLI analysis (whole-body total flux; p=0.0084, Figure 2Aii), with a concurrent 47.37% reduction in serum paraprotein levels (p=0.0382; Figure 2Aiii). In mice bearing Vk*Myc tumours, there was a 15.2% decrease in tumour burden as determined by circulating serum paraprotein (p=0.0055; Figure 2Bii) as well as a 31.4% decrease in BM tumour burden (p=0.0468; Figure 2Biii) in AZD5904-treated mice, when compared with vehicle-treated controls. Contrastingly, when AZD5904 treatment was initiated at the first sign of detectable disease, as determined by BLI or serum paraprotein in the KaLwRij/5TGM1 and Vk*Myc models, respectively, no change in tumour burden was observed (Supplementary Figure 1, Supplementary Figure 2). Analysis of circulating immune populations (Supplementary Figure 3) and markers of liver damage (Supplementary Figure 4) confirmed that AZD5904 has no toxic effects at this dose.

AZD5904 reduces $PD1^+$ $CD8^+$ T cells in tumour bearing mice

In addition to MPO's well described role in host defence, we and others have shown that MPO influences the adaptive immune response.[11,19,20] Therefore, we investigated the effect of AZD5904 administration over the course of MM disease development on T cell populations *in vivo.* Initially, we confirmed that $PD1^+$ T cells are increased in 5TGM1 tumour-bearing mice within both the $CD4^+$ and $CD8^+$ populations in the BM (1.45-fold, p=0.0114; and 3.09-fold, p=0.0004 respectively; Figure 3A) and spleen (1.58-fold, p=0.0493; and 1.40-fold, p=0.079 respectively; Figure 3B) compared with naïve counterparts. No significant differences in PD1 expression were seen in either BM or splenic $CD4^+$ T cell populations from vehicle or AZD5904 treated mice. However, AZD5904 treatment resulted in a significant reduction in $PD1^+$ T cells within the $CD8^+$ splenic population (-1.98 fold, 0.0493; Figure 3D), with a similar trend observed in the BM (-2.49-fold, p=0.1232; Figure 3C).

Inhibition of MPO with AZD5904 rescues cytotoxic potential of T cells

We have previously shown that *ex vivo* culture of MACS separated, naïve $CD8^+$ T cells with hMPO results in decreased cytotoxic capacity.[11] Importantly, mouse and human MPO Share approximately 90% homology, conserving the catalytic activity targeted by AZD5904.[21] Here, we confirm that

AZD5904 significantly reduces the immunosuppressive effects of MPO on murine $CD8^+$ T cells in a dose dependent manner *ex vivo* (p=0.0002; Figure 4A). Despite complete restoration of cytotoxicity not being achieved with 100 µM AZD5904, we confirm that 100 µM AZD5904 completely inhibits the catalytic activity of MPO *in vitro* (Figure 4B), suggesting that the immunosuppressive actions of MPO cannot exclusively be attributed to its catalytic function.

MPO indirectly impacts MM PC sensitivity to bortezomib through interactions with BM-MSCs

The BMME is known to play a critical role in chemoprotection and enhanced survival of MM PCs.[22] More specifically, BM-MSCs isolated from MM patients provide increased chemoprotection of MM PCs compared to those from healthy donors.[23] Notably, we and others have demonstrated the capacity of MPO to modify BMME components, which can in turn facilitate MM PC growth, survival and drug resistance.[11,24,25] To this end, we examined whether MPO plays a role in regulating MM PC chemoprotection *in vitro* through regulation of BM-MSCs. Whilst MPO alone had no direct effect on 5TGM1 response to bortezomib in monoculture (Figure 5A), we observe a significant increase in the number of live 5TGM1 MM PC when cultured with BM-MSCs stimulated with MPO compared to vehicle control following treatment with 1 nM (14.3% increase; p=0.0070) and 2.5 nM (12.5% increase; p=0.0195) of bortezomib. No difference was observed when treated with 5 nM and 10 nM bortezomib (Figure 5B).

Targeted MPO inhibition does not further potentiate the anti-tumour effects of bortezomib in the KaLwRij/5TGM1 model of MM.

In order to achieve the most durable responses in MM patients, frontline therapeutics are routinely utilised in a combinatorial approach.[26] Having demonstrated that targeted inhibition of MPO, using two mechanistically distinct irreversible inhibitors, 4-ABAH[11] and AZD5904, significantly impedes MM tumour progression when treatment is initiated at the time of tumour cell inoculation, we investigated the use of MPO inhibitors in combination with bortezomib in C57BL/KaLwRij mice with established 5TGM1 tumour. AZD5904 treatment in combination with bortezomib had no observable impact on MM progression compared to bortezomib alone (whole-body total flux; p= 0.981 and SPEP; p= 0.966; Figure 6A-B). Notably, 4-ABAH in combination with bortezomib resulted in comparable results (Supplementary Figure 5).

Myeloid cells and *Mpo* expression remain elevated following bortezomib induction therapy

Whilst proteasome inhibition is a standard strategy in MM treatment, it has also been reported to impact the tumour microenvironment, inducing a pro-inflammatory landscape triggering a cascade of host-driven pro-inflammatory effects in response to treatment which may limit anti-tumour efficacy.[27,28] Here, we treated 5TGM1 tumour-bearing mice with 1 mg/kg bortezomib, which successfully ablated measurable tumour (Figure 7A). Assessment of the BM myeloid cell

compartment of tumour-bearing mice following treatment with bortezomib in the present study indicated a 22.6% increase in $CD11b^+$ myeloid cells within the BM of bortezomib treated mice compared with those receiving a vehicle control (Figure 7Bi). However, this increase was not attributed to the enrichment of monocytic ($CD11b^+Ly6G^{neg}Ly6C^+$) or granulocytic ($CD11b^+Ly6c^{int}Ly6g^+$) populations specifically (Figure 7Bii). Additionally, we observe no change in *Mpo* mRNA expression in $CD11b^+$ cells isolated from bortezomib treated mice, or circulating MPO compared to those isolated from vehicle treated, tumour-bearing mice (Figure 7C-D). Critically, however, we have previously reported that *Mpo* expression is highly expressed in myeloid cells from MM tumour bearing mice.[11] Together, these data suggest that Mpo remains at an elevated level following bortezomib treatment, despite a reduction in tumour burden. Notably, bortezomib alone had no observable effect on myeloid populations in the BM of tumour-naïve mice (Supplementary Figure 6), suggesting the increase in myeloid cells is specific to the treated tumour context.

AZD5904 delays 5TGM1 tumour relapse following treatment with bortezomib

Recurrent MM relapse remains a significant clinical challenge and largely determines long term patient outcomes. The introduction of maintenance therapy regimens following induction therapy and ASCT has resulted in a more prolonged response.[29] While the immunomodulatory drug (IMiD), lenalidomide, is routinely used as a monotherapy in patients who achieve a state of MRD-negativity, recent studies have explored combinatory and alternative approaches to achieve more durable responses to invoke more prolonged progression free survival (PFS).[30] Given we show that the bortezomib-treated BMME is “primed” with increased myeloid cells and a sustained elevation in *Mpo* expression, and inhibition of Mpo initiated prior to significant tumour establishment is effective at slowing MM progression, we hypothesised that MPO inhibition after cessation of bortezomib treatment would prevent the outgrowth of residual MM PC and hence delay relapse. To investigate this, we treated 5TGM1 tumour-bearing C57BL/KaLwRij mice with a high dose of bortezomib (1 mg/kg, i.v) during mid-stage tumour development (day 18) to achieve disease remission, with tumour being undetectable by BLI. Six days later (day 24), once bioluminescent imaging confirmed MRD-negativity, we initiated twice daily treatment with AZD5904. Strikingly, mice treated with AZD5904 exhibited a 68.1% reduction in tumour burden 13 days following bortezomib treatment cessation compared to mice treated with vehicle control ($p=0.0069$; mean BLI; vehicle, $1.01x10^7 \pm 4.21x10^6$ photons/sec, compared with treatment with AZD5904, $3.22x10^6 \pm 8.58x10^5$ photons/sec; Figure 8C).

Discussion

Growing evidence highlights the complex interplay between MM PCs and the BMME, demonstrating that extrinsic factors critically influence MM progression by modulating cell proliferation, survival, and drug resistance.[31,32] This has spurred interest in identifying microenvironmental factors as potential therapeutic targets.[4,33,34] Concurrently, combination therapies involving mechanistically distinct agents have consistently demonstrated superior outcomes in cancer treatment.[35] Given the critical role of the microenvironment in disease progression and drug resistance, there is a clear need for therapeutic strategies that simultaneously target MM PCs and modulate the BMME. Such dual-targeted approaches have the potential to achieve deeper, more durable responses and ultimately improve patient outcomes.

MPO plays diverse roles in inflammation and cancer due to its ability to interact with numerous cell types including fibroblasts, endothelial and immune cells.[4,34] Here, we have validated our previous findings identifying MPO as a viable therapeutic target, limited to early stages of disease, and mice with MRD-negativity following bortezomib treatment, using the novel, bioavailable MPO inhibitor AZD5904. Mechanistically, MPO is highly upregulated in preclinical models of MM, promoting disease progression through modulation of BM cellular components.[11] Importantly, in pancreatic cancer, where MPO is markedly overexpressed, an in vivo study found that MPO inhibition produced a dramatic reduction in myeloid cells, exhausted CD8+ T cells, and regulatory T cell subsets within the tumour microenvironment, highlighting MPO as a potent immunomodulatory target.[36] Notably, T cell populations in MM patients are well described to express markers associated with T cell exhaustion and senescence, including PD-1, CTLA-4, 2B4, CD160 and CD57, leading to impaired proliferative capacity, reduced cytokine production, and weakened antitumour cytotoxicity.[37] Indeed, we show that 5TGM1 tumour bearing mice exhibit increased PD-1^{+}CD8^{+} T cells, and targeted MPO inhibition via AZD5904 treatment results in decreased PD-1^{+}CD8^{+} T cells in 5TGM1 tumour bearing mice compared to vehicle control, suggesting MPO contributes to T cell exhaustion. Furthermore, PD-1^{+}CD8^{+} T cells in MM tumour-bearing mice have previously been reported to produce decreased levels of cytokines, including IFN-γ[38], and we have previously demonstrated that MPO reduces the proportion of IFN-γ^{+} splenocytes *ex vivo* when cultured in the presence of 5TGM1 cells.[11] Our data show that AZD5904 reverses the MPO-induced decrease in CD8^{+} T cell cytotoxicity against 5TGM1 cells in a dose dependent manner *ex vivo*. Therefore, although the reduced tumour in AZD5904 treated mice may account for changes in the expression of T cell exhaustion markers, we also provide evidence that MPO is likely to have a direct effect on T cell activity. In the present study, the activation of naïve C57BL/KaLwRij T cells by exposure to 5TGM1 cells *ex vivo* was impaired by prior culture with MPO. This suggests that MPO may invoke its immunosuppressive capabilities by impeding T cell receptor (TCR) mediated activation signals. Given PD-1 is rapidly induced on T cells

following TCR mediated activation,[39] investigation into the effect of MPO on TCR activation and subsequent proliferation and differentiation in the context of MM may provide further insight into this mechanism. Overarchingly, these data suggest that AZD5904 treatment may be a viable means to impede MPO-mediated regulation of PD-1 expression in $CD8^+$ T cells and presents as a promising immunomodulatory approach. However, further investigation is needed to define how the broader effect AZD5904 reshapes the MM immune landscape in both established disease and following bortezomib treatment, and to elucidate the mechanisms by MPO activity enhances T cell exhaustion and immune suppression.

Innate and acquired resistance remain major challenges in MM treatment.[40] While intrinsic adaptations in MM PCs promote survival against therapeutics, the BMME also contributes to disease persistence.[23,41] Specifically, BM stromal populations, including fibroblasts and PMN-MDSCs, support MM PC survival during chemotherapy treatment.[42] MPO directly regulates fibroblast and PMN activity, enhancing matrix formation and stimulating BM-MSC expression of pro-growth and survival factors.[4,11,24,42] In this study, BM-MSCs from C57Bl/KaLwRij mice stimulated with hMPO supported 5TGM1 survival/proliferation following bortezomib treatment, suggesting MPO may augment the chemoprotective capacity of BM-MSCs. However, despite these *in vitro* findings, MPO inhibition, did not impede tumour progression when treatment was initiated after disease establishment, or enhance the antitumor effects of bortezomib. Whilst it cannot be ruled out that the pharmacokinetics of the agents used and the schedules utilised through these models may act as a contributing factor to the lack of efficacy observed in the present study, it is likely that these findings suggest that MPO plays a more prominent role during early disease establishment rather than in established disease when PC burden is high. Indeed, MM progression involves a gradual shift in growth factor dependence, with MM PCs becoming less reliant on external growth factors in advanced disease.[44] In support of this, the specific targeting of MSC secreted Gremlin1 in the KaLwRij/5TGM1 model resulted in a significant decrease in MM tumour progression when treatment was initiated at the time of tumour inoculation, but not when treatment was initiated in an established disease context.[15] These findings represent a key insight regarding the timing of MPO inhibition and other emerging BMME-targeted strategies in MM, specifically highlighting their optimal use likely falls during early disease stages such as MGUS or smouldering MM, or as part of a maintenance approach following induction therapy to prevent or delay MM PC outgrowth and relapse.

The current reality facing patients is that even those who achieve a high quality and prolonged duration of response with initial therapy will ultimately relapse, thus, improving management of relapsed disease is a critical aspect of MM treatment. Chemotherapeutic agents have been shown to modify the tumour microenvironment, which can promote tumour recurrence even while eliciting direct anti-cancer effects.[45] For example, preclinical models of breast and lung cancer have been

reported to induce matrix metalloproteinase-9 and VEGFR-1 expression following chemotherapy, aiding in tumour cell metastasis and homing.[46,47] Although the primary means by which proteasome inhibitors, such as bortezomib, induce MM PC death is through the ER stress response, their mechanism of action has been described to extend further, interacting with extrinsic components of the BMME including osteoblasts, osteoclasts and T cells [48-50], with some of these interactions leading to the creation of a pro-tumorigenic landscape that remains following treatment cessation. Specifically, Beyar-Katz and colleagues report that bortezomib induces a cascade of host-driven pro-inflammatory responses which may limit its anti-tumour efficacy in MM.[27] This study showed that systemic bortezomib treatment in SCID mice injected with CAG cells, not only results in accumulation of macrophages at sites of tumour, which have been shown to shown to play a chemoprotective role, but also an increase in the critical myeloma growth factor IL6.[27] We have previously reported MM tumour progression in the KaLwRij/5TGM1 model to be associated with elevated expression of *Mpo* from $Cd11b^+$ myeloid cells within the BMME.[11] Here we demonstrate that 5TGM1 tumour-bearing mice treated with bortezomib maintain the elevated levels of $CD11b^+$-derived *Mpo* mRNA expression and high levels of circulating MPO, despite the ablation of tumour. Furthermore, bortezomib treatment of tumour naïve mice had no significant impact on BM $CD11b^+$ populations and accompanying *Mpo* expression, suggesting that myeloid cell changes within the BM are not directly mediated by bortezomib alone. Collectively these data indicate that bortezomib induced MM cell death amplifies, or at the least sustains, the pro-inflammatory and pro-tumorigenic state of the BM microenvironment. This primed niche represents an encouraging therapeutic target with the potential to modulate the immune and cellular mechanisms that drive MM relapse. In support of this, we demonstrate that AZD5904 treatment considerably impedes MM PC outgrowth after achieving tumour remission using bortezomib.

Currently, IMiDs such as lenalidomide, are fundamental to MM management, particularly as maintenance therapy, due to their ability to target both malignant plasma cells and various components of the MM BMME.[51] While IMiDs offer substantial clinical benefits in curbing relapse, long-term therapy can be associated with manageable but sometimes significant side effects, reinforcing the ongoing need for diversified and personalized maintenance strategies that might offer improved tolerability or target specific relapse mechanisms.[52] Additionally, a recent study by Badros and colleagues explored the use of daratumumab, a human immunoglobulin G kappa monoclonal antibody targeting CD38, and lenalidomide following ASCT, and found a significant improvement in PFS with no reported concerns regarding safety compared to lenalidomide alone.[53] Given the favourable safety, tolerability, and pharmacokinetic profile of MPO inhibitors in humans[54], further investigation of MPO inhibitors such as AZD5904 is warranted as a complementary therapeutic approach.

Conclusion

In conclusion, this study evaluated the potential of MPO inhibition as a strategic addition to MM treatment in combination with the frontline proteasome inhibitor, bortezomib. Although administration of AZD5904 in established disease did not provide benefit as a monotherapy, or enhance the effects of bortezomib when used in combination, our results demonstrate that AZD5904 significantly attenuates MM relapse following bortezomib induction therapy. Considering that disease relapse remains a persistent challenge for patients and clinicians, these findings underscore the promising role of MPO inhibitors as a candidate for maintenance therapy. Future research should evaluate their efficacy and potential integration into comprehensive MM treatment regimens.

References

1. Eisfeld C, Kajuter H, Moller L, Wellmann I, Shumilov E, Stang A. Time trends in survival and causes of death in multiple myeloma: a population-based study from Germany. BMC Cancer. 2023;23(1):317.
2. Laubach J, Garderet L, Mahindra A, et al. Management of relapsed multiple myeloma: recommendations of the International Myeloma Working Group. Leukemia. 2016;30(5):1005-1017.
3. Majithia N, Rajkumar SV, Lacy MQ, et al. Early relapse following initial therapy for multiple myeloma predicts poor outcomes in the era of novel agents. Leukemia. 2016;30(11):2208-2213.
4. Panagopoulos V, Leach DA, Zinonos I, et al. Inflammatory peroxidases promote breast cancer progression in mice via regulation of the tumour microenvironment. Int J Oncol. 2017;50(4):1191-1200.
5. Rymaszewski AL, Tate E, Yimbesalu JP, et al. The role of neutrophil myeloperoxidase in models of lung tumor development. Cancers (Basel). 2014;6(2):1111-1127.
6. Youn JI, Collazo M, Shalova IN, Biswas SK, Gabrilovich DI. Characterization of the nature of granulocytic myeloid-derived suppressor cells in tumor-bearing mice. J Leukoc Biol. 2012;91(1):167-181.
7. Romano A, Conticello C, Cavalli M, et al. Immunological dysregulation in multiple myeloma microenvironment. Biomed Res Int. 2014;2014:198539.
8. Gorgun GT, Whitehill G, Anderson JL, et al. Tumor-promoting immune-suppressive myeloid-derived suppressor cells in the multiple myeloma microenvironment in humans. Blood. 2013;121(15):2975-2987.
9. Ramachandran IR, Martner A, Pisklakova A, et al. Myeloid-derived suppressor cells regulate growth of multiple myeloma by inhibiting T cells in bone marrow. J Immunol. 2013;190(7):3815-3823.
10. Malek E, de Lima M, Letterio JJ, et al. Myeloid-derived suppressor cells: The green light for myeloma immune escape. Blood Rev. 2016;30(5):341-348.
11. Williams CMD, Noll JE, Bradey AL, et al. Myeloperoxidase creates a permissive microenvironmental niche for the progression of multiple myeloma. Br J Haematol. 2023;203(4):614-624.
12. Tiden AK, Sjogren T, Svensson M, et al. 2-thioxanthines are mechanism-based inactivators of myeloperoxidase that block oxidative stress during inflammation. J Biol Chem. 2011;286(43):37578-37589.
13. Churg A, Marshall CV, Sin DD, et al. Late intervention with a myeloperoxidase inhibitor stops progression of experimental chronic obstructive pulmonary disease. Am J Respir Crit Care Med. 2012;185(1):34-43.
14. Clark KC, Hewett DR, Panagopoulos V, et al. Targeted Disruption of Bone Marrow Stromal Cell-Derived Gremlin1 Limits Multiple Myeloma Disease Progression In Vivo. Cancers (Basel). 2020;12(8):2149.
15. Bradey AL, Fitter S, Duggan J, et al. Calorie restriction has no effect on bone marrow tumour burden in a Vk*MYC transplant model of multiple myeloma. Sci Rep. 2022;12(1):13128.
16. Mrozik KM, Cheong CM, Hewett D, et al. Therapeutic targeting of N-cadherin is an effective treatment for multiple myeloma. Br J Haematol. 2015;171(3):387-399.

17. Wang Z, Zhang L, Wang H, et al. Tumor-induced CD14+HLA-DR (-/low) myeloid-derived suppressor cells correlate with tumor progression and outcome of therapy in multiple myeloma patients. Cancer Immunol Immunother. 2015;64(3):389-399.
18. Regard JB, Harrison TJ, Axford J, et al. Discovery of a novel, highly potent and orally bioavailable pyrrolidinone indole series of irreversible Myeloperoxidase (MPO) inhibitors. Biochem Pharmacol. 2023;209:115418.
19. Odobasic D, Kitching AR, Yang Y, et al. Neutrophil myeloperoxidase regulates T-cell-driven tissue inflammation in mice by inhibiting dendritic cell function. Blood. 2013;121(20):4195-4204.
20. Valadez-Cosmes P, Maitz K, Kindler O, et al. Myeloperoxidase promotes a tumorigenic microenvironment in non-small cell lung cancer. bioRxiv. 2023;2023.2001.2028.526014 [preprint, not peer-reviewed].
21. Erdbrugger U, Hellmark T, Bunch DO, et al. Mapping of myeloperoxidase epitopes recognized by MPO-ANCA using human-mouse MPO chimers. Kidney Int. 2006;69(10):1799-1805.
22. Bhowmick K, von Suskil M, Al-Odat OS, et al. Pathways to therapy resistance: The sheltering effect of the bone marrow microenvironment to multiple myeloma cells. Heliyon. 2024;10(12):e33091.
23. Yang H, Zheng Y, Zhang Y, Cao Z, Jiang Y. Mesenchymal stem cells derived from multiple myeloma patients protect against chemotherapy through autophagy-dependent activation of NF-kappaB signaling. Leuk Res. 2017;60:82-88.
24. Harmer D, Falank C, Reagan MR. Interleukin-6 Interweaves the Bone Marrow Microenvironment, Bone Loss, and Multiple Myeloma. Front Endocrinol. (Lausanne). 2018;9:788.
25. Tancred TM, Belch AR, Reiman T, Pilarski LM, Kirshner J. Altered expression of fibronectin and collagens I and IV in multiple myeloma and monoclonal gammopathy of undetermined significance. J Histochem Cytochem. 2009;57(3):239-247.
26. Rajkumar SV, Kumar S. Multiple myeloma current treatment algorithms. Blood Cancer J. 2020;10(9):94.
27. Beyar-Katz O, Magidey K, Ben-Tsedek N, et al. Bortezomib-induced pro-inflammatory macrophages as a potential factor limiting anti-tumour efficacy. J Pathol. 2016;239(3):262-273.
28. Cullen SJ, Ponnappan S, Ponnappan U. Proteasome inhibition up-regulates inflammatory gene transcription induced by an atypical pathway of NF-kappaB activation. Biochem Pharmacol. 2010;79(5):706-714.
29. McCarthy PL, Holstein SA, Petrucci MT, et al. Lenalidomide Maintenance After Autologous Stem-Cell Transplantation in Newly Diagnosed Multiple Myeloma: A Meta-Analysis. J Clin Oncol. 2017;35(29):3279-3289.
30. Patel KK, Shah JJ, Feng L, et al. Safety and Efficacy of Combination Maintenance Therapy with Ixazomib and Lenalidomide in Patients with Posttransplant Myeloma. Clin Cancer Res. 2022;28(7):1277-1284.
31. Abdi J, Chen G, Chang H. Drug resistance in multiple myeloma: latest findings and new concepts on molecular mechanisms. Oncotarget. 2013;4(12):2186-2207.
32. Kawano Y, Moschetta M, Manier S, et al. Targeting the bone marrow microenvironment in multiple myeloma. Immunol Rev. 2015;263(1):160-172.

33. Kubala L, Kolarova H, Vitecek J, et al. The potentiation of myeloperoxidase activity by the glycosaminoglycan-dependent binding of myeloperoxidase to proteins of the extracellular matrix. Biochim Biophys Acta. 2013;1830(10):4524-4536.
34. Panagopoulos V, Zinonos I, Leach DA, et al. Uncovering a new role for peroxidase enzymes as drivers of angiogenesis. Int J Biochem Cell Biol. 2015;68:128-138.
35. Bayat Mokhtari R, Homayouni TS, Baluch N, et al. Combination therapy in combating cancer. Oncotarget. 2017;8(23):38022-38043.
36. Basnet A, Landreth KM, Nohoesu R, et al. Targeting myeloperoxidase limits myeloid cell immunosuppression enhancing immune checkpoint therapy for pancreatic cancer. Cancer Immunol Immunother. 2024;73(3):57.
37. Zelle-Rieser C, Thangavadivel S, Biedermann R, et al. T cells in multiple myeloma display features of exhaustion and senescence at the tumor site. J Hematol Oncol. 2016;9(1):116.
38. Hallett WH, Jing W, Drobyski WR, Johnson BD. Immunosuppressive effects of multiple myeloma are overcome by PD-L1 blockade. Biol Blood Marrow Transplant. 2011;17(8):1133-1145.
39. Chikuma S, Terawaki S, Hayashi T, et al. PD-1-mediated suppression of IL-2 production induces CD8+ T cell anergy in vivo. J Immunol. 2009;182(11):6682-6689.
40. Uckun FM. Cancer drug resistance in multiple myeloma. Cancer Drug Resist. 2022;5(2):271-276.
41. Zhang G, Miao F, Xu J, Wang R. Mesenchymal stem cells from bone marrow regulate invasion and drug resistance of multiple myeloma cells by secreting chemokine CXCL13. Bosn J Basic Med Sci. 2020;20(2):209-217.
42. Ria R, Vacca A. Bone Marrow Stromal Cells-Induced Drug Resistance in Multiple Myeloma. Int J Mol Sci. 2020;21(2):613.
43. DeNichilo MO, Panagopoulos V, Rayner TE, Borowicz RA, Greenwood JE, Evdokiou A. Peroxidase enzymes regulate collagen extracellular matrix biosynthesis. Am J Pathol. 2015;185(5):1372-1384.
44. Moser-Katz T, Joseph NS, Dhodapkar MV, Lee KP, Boise LH. Game of Bones: How Myeloma Manipulates Its Microenvironment. Front Oncol. 2020;10:625199.
45. Vorontsova A, Kan T, Raviv Z, Shaked Y. The Dichotomous Role of Bone Marrow Derived Cells in the Chemotherapy-Treated Tumor Microenvironment. J Clin Med. 2020;9(12):3912.
46. Daenen LG, Roodhart JM, van Amersfoort M, et al. Chemotherapy enhances metastasis formation via VEGFR-1-expressing endothelial cells. Cancer Res. 2011;71(22):6976-6985.
47. Gingis-Velitski S, Loven D, Benayoun L, et al. Host response to short-term, single-agent chemotherapy induces matrix metalloproteinase-9 expression and accelerates metastasis in mice. Cancer Res. 2011;71(22):6986-6996.
48. Boissy P, Andersen TL, Lund T, Kupisiewicz K, Plesner T, Delaisse JM. Pulse treatment with the proteasome inhibitor bortezomib inhibits osteoclast resorptive activity in clinically relevant conditions. Leuk Res. 2008;32(11):1661-1668.
49. Giuliani N, Morandi F, Tagliaferri S, et al. The proteasome inhibitor bortezomib affects osteoblast differentiation in vitro and in vivo in multiple myeloma patients. Blood. 2007;110(1):334-338.
50. Gulla A, Morelli E, Samur MK, et al. Bortezomib induces anti-multiple myeloma immune response mediated by cGAS/STING pathway activation. Blood Cancer Discov. 2021;2(5):468-483.

51. Holstein SA, McCarthy PL. Immunomodulatory Drugs in Multiple Myeloma: Mechanisms of Action and Clinical Experience. Drugs. 2017;77(5):505-520.
52. Buck C, Brenes Castillo F, Bettio E, et al. The impact of continuous lenalidomide maintenance treatment on people living with multiple myeloma-a single-centre, qualitative service evaluation study. Support Care Cancer. 2024;32(7):479.
53. Badros A, Foster L, Anderson LD Jr, et al. Daratumumab with lenalidomide as maintenance after transplant in newly diagnosed multiple myeloma: the AURIGA study. Blood. 2025;145(3):300-310.
54. Gan LM, Lagerstrom-Fermer M, Ericsson H, et al. Safety, tolerability, pharmacokinetics and effect on serum uric acid of the myeloperoxidase inhibitor AZD4831 in a randomized, placebo-controlled, phase I study in healthy volunteers. Br J Clin Pharmacol. 2019;85(4):762-770.

Figure Legends

Figure 1. Mpo is systemically increased in MM tumour bearing mice. A) (i) Representative BLI images of 5TGM1 tumour-bearing C57BL/KaLwRij mice, (ii) serum Mpo concentration after 21, 28 and 35 days of 5TGM1 tumour progression and (iii) tumour burden (Whole Body Total Flux; photons/ second) plotted against circulating MPO at varying tumour endpoints (naïve, day 21, day 28, day 35). **B)** (i) Serum Mpo concentration after 9 weeks of Vk*Myc tumour progression. (ii) The proportion of CD11b+ myeloid cells within the BM of naïve and Vk*Myc tumour bearing mice, at early (week 6) and late (week 9) stage tumour development, were determined by flow cytometry, represented as a percentage of non-tumour (GFPneg) BM cells, (iii) Mpo mRNA expression in MACS enriched CD11b+ cells isolated from BM of naïve or tumour-bearing (week 6 & 9) mice, normalised to Gapdh, (iv) Varying endpoint (naïve, week 6, week 9) tumour Burden (GFP percentage) in the BM plotted against BM CD11b+ Mpo expression. Box and whisker plots show the median and interquartile ranges (IQRs) between 25% (Q1) and 75% quartiles (Q3), the lower and upper whiskers indicate minimum and maximum values respectively, Shaded area represents the 95% confidence interval, n=4 mice/group (A) or n=5-6 mice/group (B). One-way ANOVA with Tukey's multiple comparisons test was used to calculate significance, *p<0.05, ***p<0.001, and ns (non-significant) (p>0.05).

Figure 2. AZD5904 treatment initiation at the time of 5TGM1 and Vk*Myc cell inoculation impedes tumour progression. Eight-week-old C57BL/KaLwRij and C57BL/6J mice were treated with AZD5904 (150 mg/kg; i.p.) twice daily, initiated 24 hours prior to tumour engraftment of 5TGM1 MM cells and Vk*Myc cells respectively (i.v.). **A)** 5TGM1/KaLwRij model (i) representative BLI images of tumour progression, (ii) longitudinal tumour burden quantified as photons per second and (iii) endpoint tumour burden measured by serum protein electrophoresis (SPEP) (day 28) normalised to internal albumin. **B)** Vk*Myc Model (i) tumour progression as determined by weekly SPEP, (ii) endpoint SPEP values of individual mice and (iii) hind limb BM tumour burden as determined by GFP percentage. Results are shown as the mean ± SEM, n=8 mice/group (A) or n=10-12 mice/group (B). Two-way ANOVA with Šídák's multiple comparisons test or unpaired t-test was used to calculate significance where appropriate, *p<0.05 and **p<0.01.

Figure 3. AZD5904 regulates T cell populations in the BM and spleen of 5TGM1 tumour bearing mice. Whole BM and spleen tissue were collected from naive and 5TGM1 tumour bearing **(A, B)**, as well as vehicle and AZD5904 treated 5TGM1 tumour-bearing mice **(C, D)** at experimental endpoint (day 29) to assess proportions of $PD1^+$ populations within $CD3^+CD4^+$ and $CD3^+CD8^+$ populations by flow cytometric analysis. Results are shown as the mean ± SEM, n=4-8 mice/group.

Unpaired t-test was used to calculate significance, *p<0.05, **p<0.01, ***p<0.001 and ns (non-significant) (p>0.05).

Figure 4. AZD5904 rescues CD8$^+$ T cell cytotoxic potential. A) CD8$^+$ T cell (C57BL/KaLwRij) cytotoxicity (irradiated-5TGM1 MM cells) after 24 hours of culture in the presence or absence of MPO (2 µg/mL) and AZD5904 (20 -100µM) measured by LDH release. **B)** Percentage of luminol activity of 2 µg/mL of MPO *in vitro* with varying concentrations of AZD5904, as measured by luminal oxidation and luminescence. Results are shown as the mean ± SEM, n=3-6/group, performed in technical triplicate. One-way ANOVA with Tukey's multiple comparisons test was used to calculate significance, *p<0.05, ***p<0.001 and ns (non-significant) (p>0.05).

Figure 5. MPO promotes chemoprotective effects of BM-MSCs. A) Relative proportion of 5TGM1 cells per well, directly treated with hMPO (2 µg/mL) for 24 hours in monoculture followed by 24 hours bortezomib treatment, as determined by luminescence (relative to vehicle control). **B)** BM-MSCs were isolated from naïve C57BL/KaLwRij mice and cultured *ex vivo*. BM-MSCs were stimulated with hMPO (2 µg/mL) for 24 hours, prior to the addition of 5TGM1 MM PCs. Following 8-hours of co-culture, bortezomib was added at varying concentrations (1 nM, 2.5 nM, 5 nM and 10 nM) and cultured for a further 24 hours and the relative number of live 5TGM1 cells per well (relative to vehicle control) was determined by luminescence. Results are shown as the mean ± SEM, n=3 independent donors, run in triplicate. Two-way ANOVA with Šídák's multiple comparisons test was used to calculate significance, *p<0.05 and **p<0.01 and ns (non-significant) (p>0.05).

Figure 6. AZD5904 does not potentiate the anti-tumour effects of bortezomib. Six to eight-week-old C57BL/KaLwRij mice were treated with AZD5904 (150 mg/kg; p.o. twice daily and bortezomib (0.2 mg/kg; i.v.) twice weekly initiated 18 days following 5TGM1 cell inoculation (at first measurable sign of disease by BLI). **A)** (i) Representative BLI images, (ii) tumour burden quantified as photons per second. **B)** Endpoint tumour burden measured by serum protein electrophoresis (SPEP) (day 28) normalised to internal albumin. Results are shown as the mean ± SEM, n=8-9 mice/group. Two-way and One-way ANOVA with Šídák's multiple comparisons test or Tukey's multiple comparisons test respectively were used to calculate significance where appropriate, *p<0.05, **p<0.01 and ns (non-significant; p>0.05).

Figure 7. Myeloid cells are expanded and MPO remains upregulated in mice following high dose bortezomib induction therapy. Eight-week-old C57BL/KaLwRij mice were inoculated with 5TGM1 MM cells (i.v.). Mice received two treatments of bortezomib (1 mg/kg i.v.) after 18 days of tumour establishment. **A)** Representative images confirming an absence of 5TGM1 tumour following bortezomib administration **B)** i) The proportion of $CD11b^+$ myeloid cells within the BM (GFP negative) at experimental endpoint and ii) The ratio of granulocytes to monocytes within the total $CD11b^+$ myeloid cell population. **C)** Mpo mRNA expression in magnetically activated cell sorting (MACS)-enriched BM $CD11b^+$ cells. **D)** Endpoint serum MPO concentration. Results are shown as the mean ± SEM, n=3–5 mice/group. Unpaired t-test was used to calculate significance, **p<0.01 and ns (non-significant; p>0.05).

Figure 8. AZD5904 prolongs 5TGM1 relapse duration following treatment with bortezomib. A) Eight-week-old C57BL/KaLwRij mice were inoculated with 5TGM1 MM cells (i.v.). All mice (excluding untreated tumour control group) received two treatments of bortezomib (1 mg/kg i.v.) after 18 days of tumour establishment. Following confirmation of undetectable tumour by BLI, mice were treated with either AZD5904 (150 mg/kg; p.o.) twice daily, or vehicle until experimental endpoint. **B)** Representative ventral BLI images. **C)** Ventral tumour burden quantified as photons per second. Results are shown as the mean ± SEM, n=13-14 mice/group. Two-way ANOVA with Šídák's multiple comparisons test was used to calculate significance, **p<0.01.

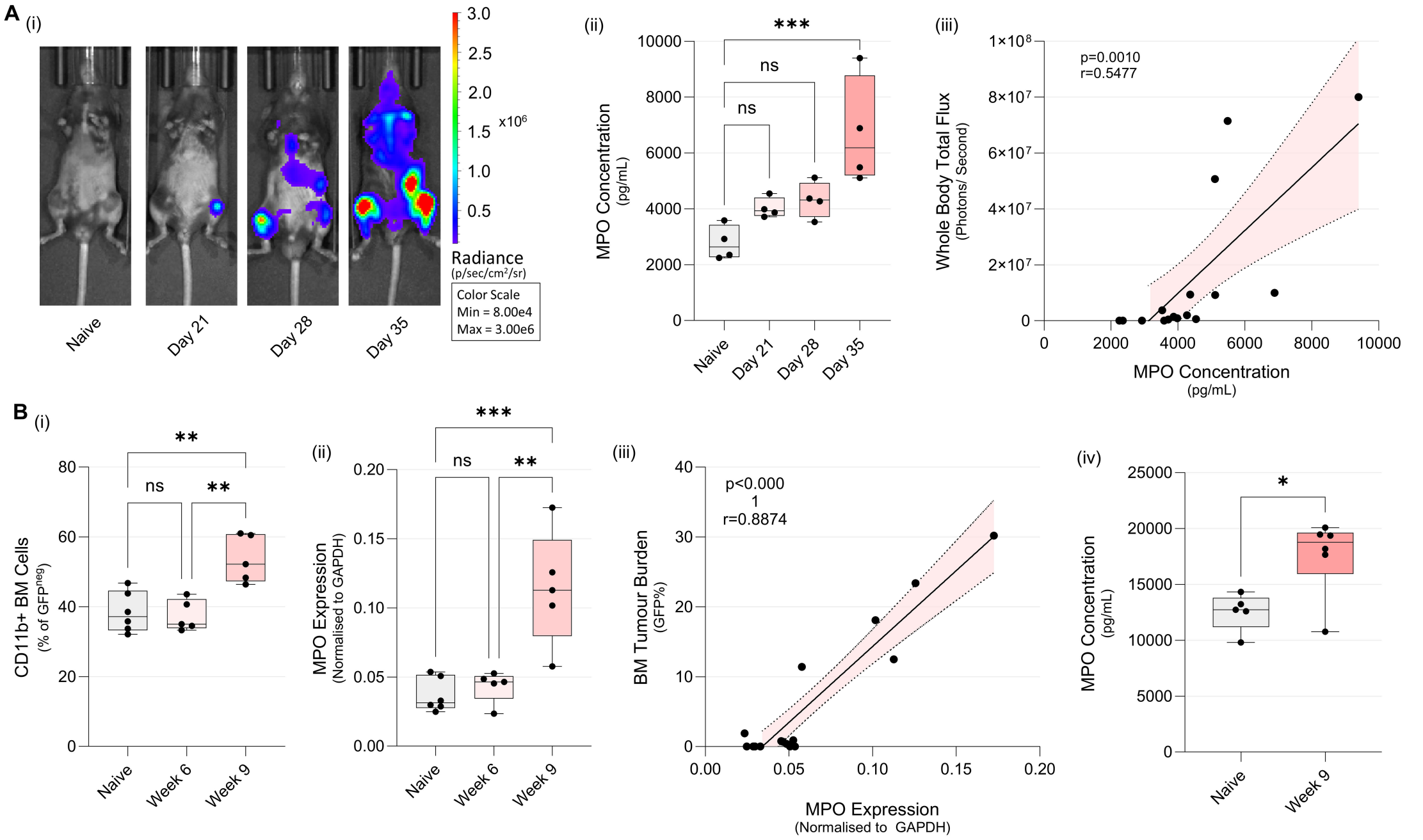
A
(i)
3.0
2.5
2.0
1.5
1.0
0.5
x10^6
Radiance
(p/sec/cm²/sr)
Color Scale
Min = 8.00e4
Max = 3.00e6
Naive
Day 21
Day 28
Day 35
(ii)
***
ns
ns
MPO Concentration
(pg/mL)
10000
8000
6000
4000
2000
0
Naive
Day 21
Day 28
Day 35
(iii)
p=0.0010
r=0.5477
Whole Body Total Flux
(Photons/ Second)
1×10^8
8×10^7
6×10^7
4×10^7
2×10^7
0
0
2000
4000
6000
8000
10000
MPO Concentration
(pg/mL)
B
(i)
**
ns
**
CD11b+ BM Cells
(% of GFP^neg)
80
60
40
20
0
Naive
Week 6
Week 9
(ii)
***
ns
**
MPO Expression
(Normalised to GAPDH)
0.20
0.15
0.10
0.05
0.00
Naive
Week 6
Week 9
(iii)
p<0.000
1
r=0.8874
BM Tumour Burden
(GFP%)
40
30
20
10
0
0.00
0.05
0.10
0.15
0.20
MPO Expression
(Normalised to GAPDH)
(iv)
*
MPO Concentration
(pg/mL)
25000
20000
15000
10000
5000
0
Naive
Week 9

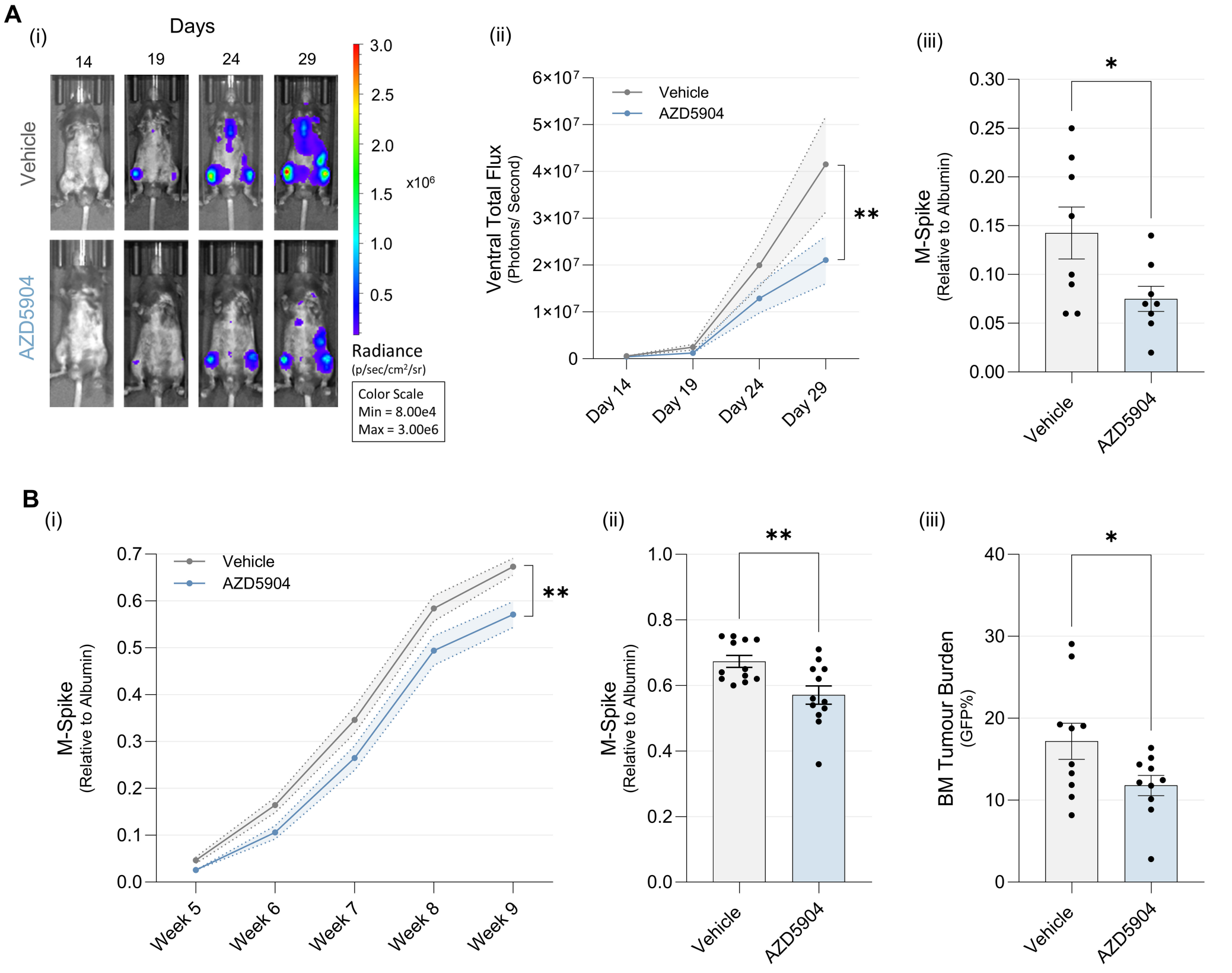
A
(i)
Days
14
19
24
29
Vehicle
AZD5904
3.0
2.5
2.0
1.5
1.0
0.5
x10⁶
Radiance
(p/sec/cm²/sr)
Color Scale
Min = 8.00e4
Max = 3.00e6
(ii)
Ventral Total Flux
(Photons/ Second)
6×10⁷
5×10⁷
4×10⁷
3×10⁷
2×10⁷
1×10⁷
0
Vehicle
AZD5904
**
Day 14
Day 19
Day 24
Day 29
(iii)
M-Spike
(Relative to Albumin)
*
0.30
0.25
0.20
0.15
0.10
0.05
0.00
Vehicle
AZD5904
B
(i)
M-Spike
(Relative to Albumin)
0.7
0.6
0.5
0.4
0.3
0.2
0.1
0.0
Vehicle
AZD5904
**
Week 5
Week 6
Week 7
Week 8
Week 9
(ii)
M-Spike
(Relative to Albumin)
**
1.0
0.8
0.6
0.4
0.2
0.0
Vehicle
AZD5904
(iii)
BM Tumour Burden
(GFP%)
*
40
30
20
10
0
Vehicle
AZD5904

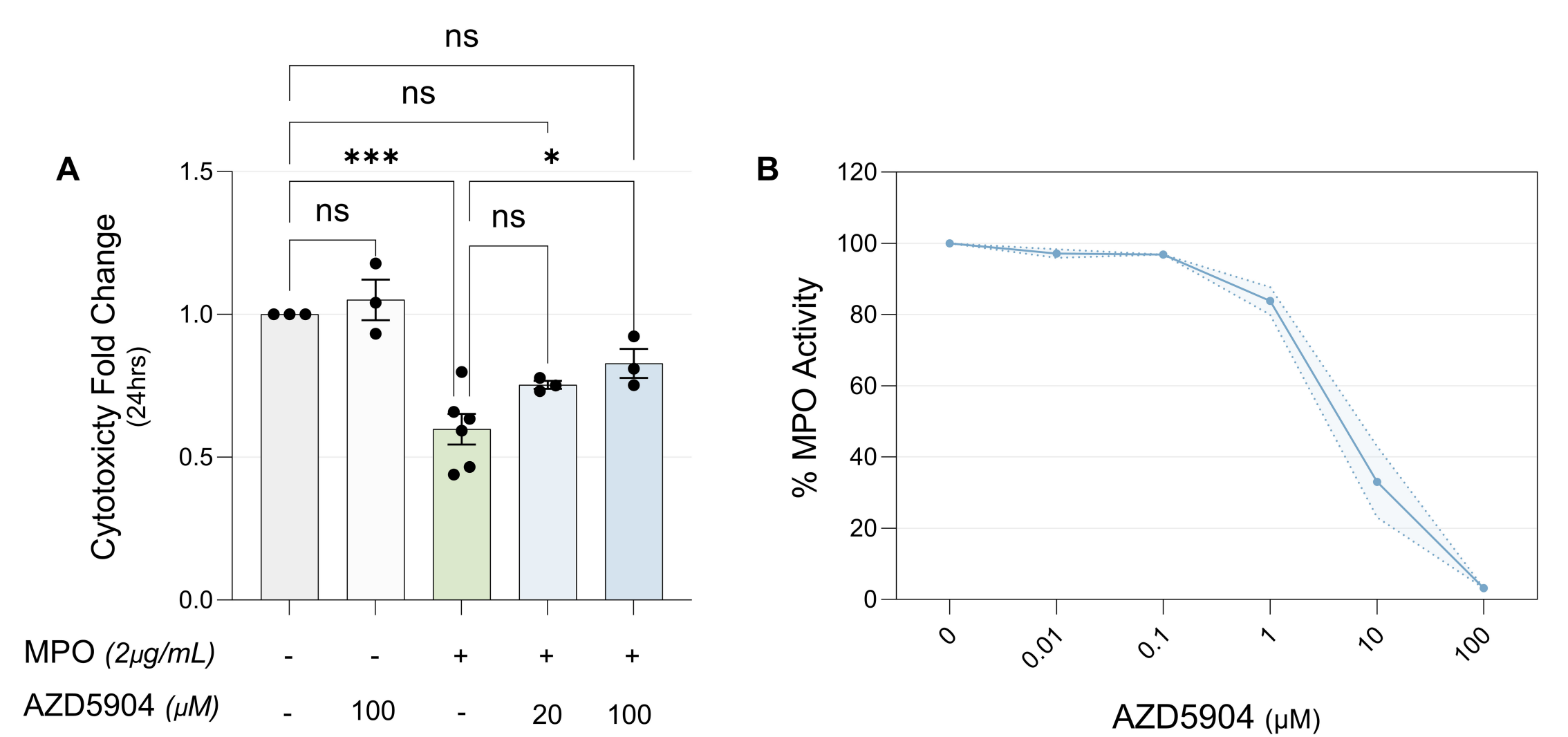
A
ns
ns
***
*
ns
ns
Cytotoxicty Fold Change
(24hrs)
1.5
1.0
0.5
0.0
MPO (2μg/mL)
- - + + +
AZD5904 (μM)
- 100 - 20 100
B
% MPO Activity
120
100
80
60
40
20
0
0
0.01
0.1
1
10
100
AZD5904 (μM)

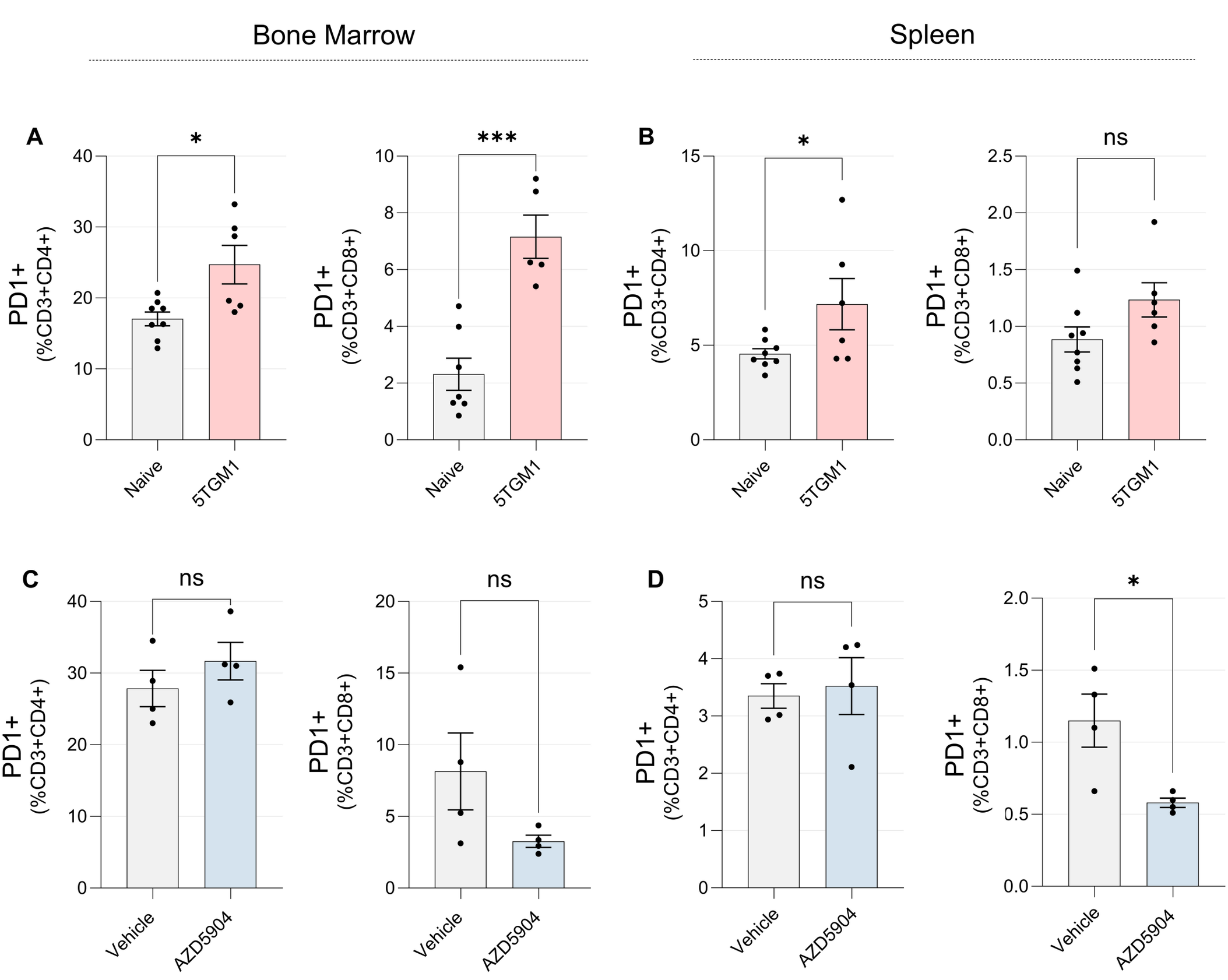
Bone Marrow
Spleen
A
B
C
D
PD1+ (%CD3+CD4+)
PD1+ (%CD3+CD8+)
*
***
ns
Naive
5TGM1
Vehicle
AZD5904

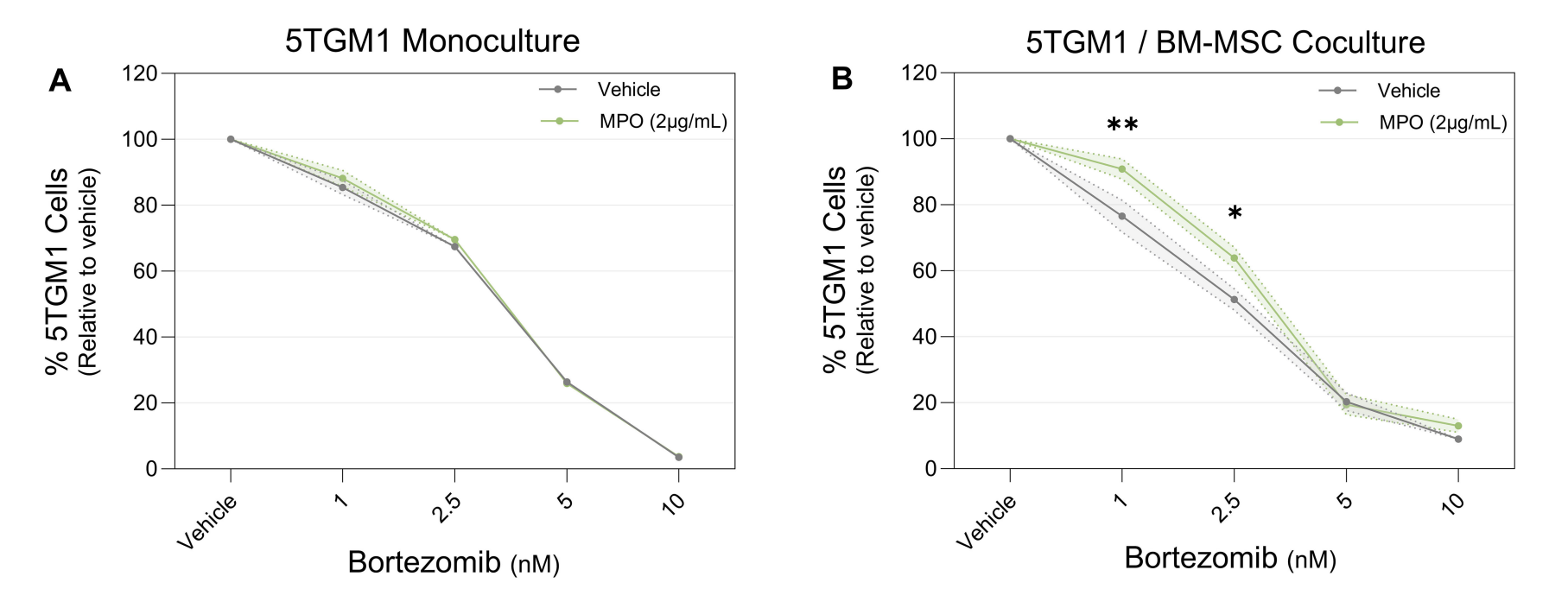
A
5TGM1 Monoculture
% 5TGM1 Cells
(Relative to vehicle)
120
100
80
60
40
20
0
Vehicle
MPO (2µg/mL)
Vehicle
1
2.5
5
10
Bortezomib (nM)
B
5TGM1 / BM-MSC Coculture
% 5TGM1 Cells
(Relative to vehicle)
**
*
Vehicle
MPO (2µg/mL)
Vehicle
1
2.5
5
10
Bortezomib (nM)

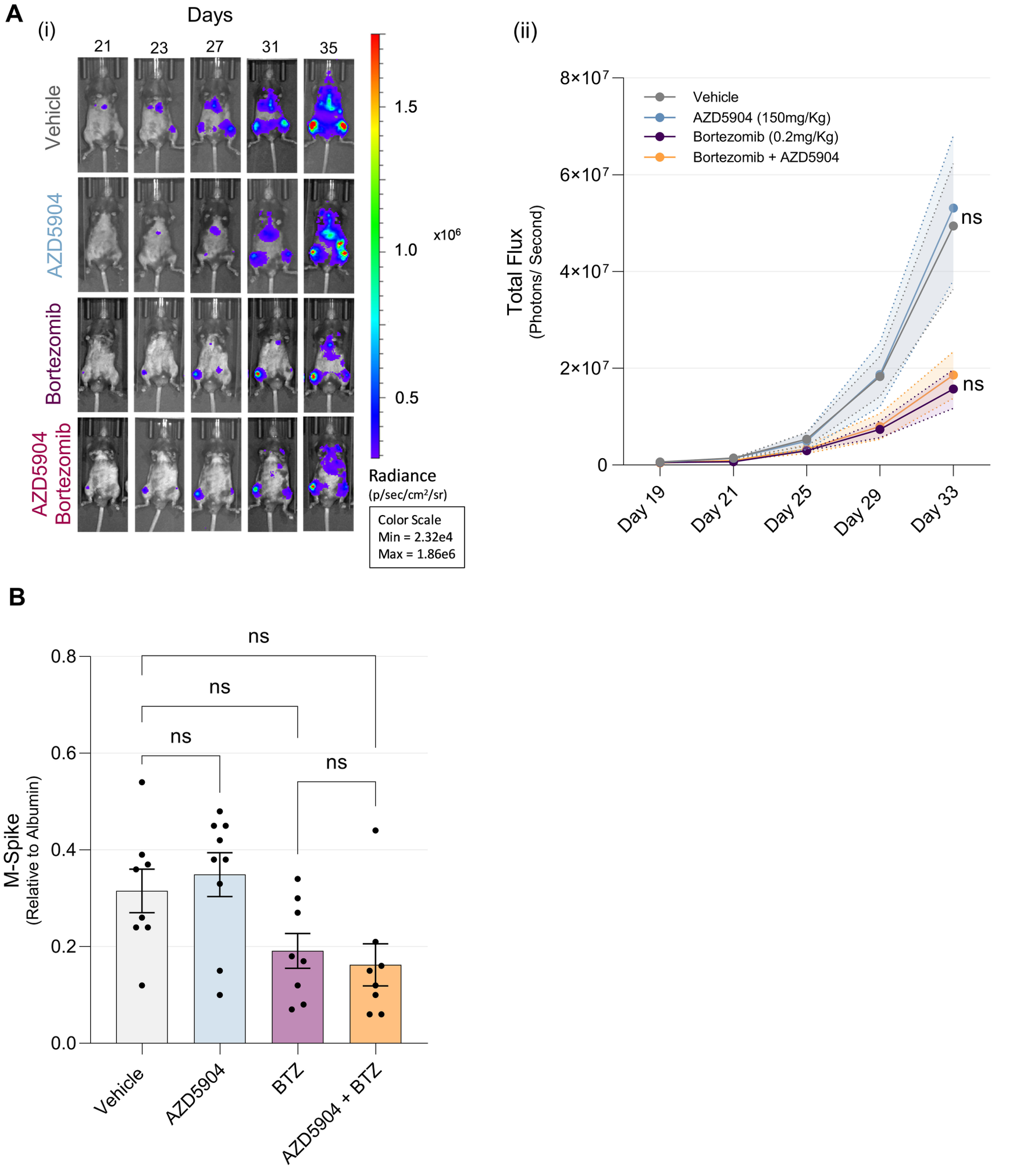
A
(i)
Days
21
23
27
31
35
Vehicle
AZD5904
Bortezomib
AZD5904
Bortezomib
1.5
1.0
0.5
x10⁶
Radiance
(p/sec/cm²/sr)
Color Scale
Min = 2.32e4
Max = 1.86e6
(ii)
Total Flux
(Photons/ Second)
8×10⁷
6×10⁷
4×10⁷
2×10⁷
0
Vehicle
AZD5904 (150mg/Kg)
Bortezomib (0.2mg/Kg)
Bortezomib + AZD5904
ns
ns
Day 19
Day 21
Day 25
Day 29
Day 33
B
M-Spike
(Relative to Albumin)
0.8
0.6
0.4
0.2
0.0
ns
ns
ns
ns
Vehicle
AZD5904
BTZ
AZD5904 + BTZ

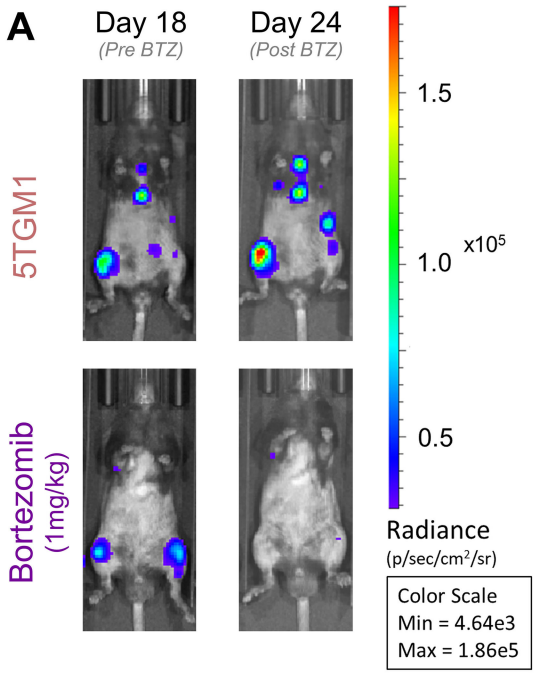
A
Day 18
(Pre BTZ)
Day 24
(Post BTZ)
5TGM1
Bortezomib
(1mg/kg)
1.5
1.0
x10^5
0.5
Radiance
(p/sec/cm²/sr)
Color Scale
Min = 4.64e3
Max = 1.86e5

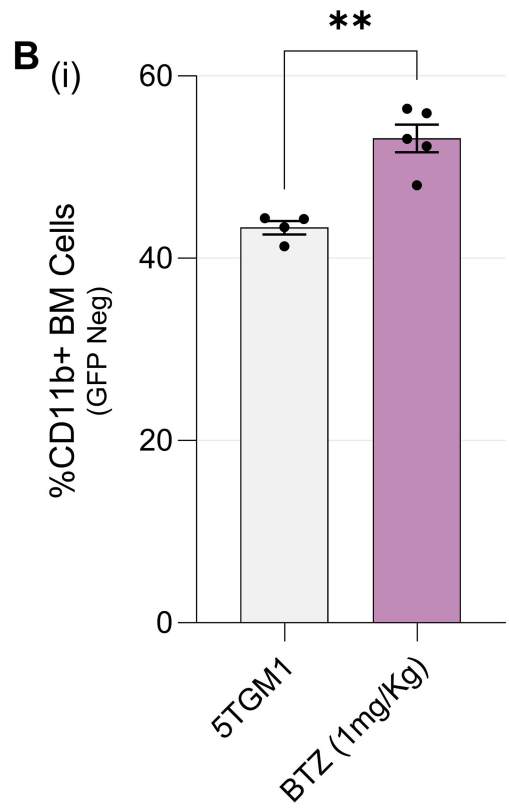
B
(i)
**
%CD11b+ BM Cells
(GFP Neg)
60
40
20
0
5TGM1
BTZ (1mg/Kg)

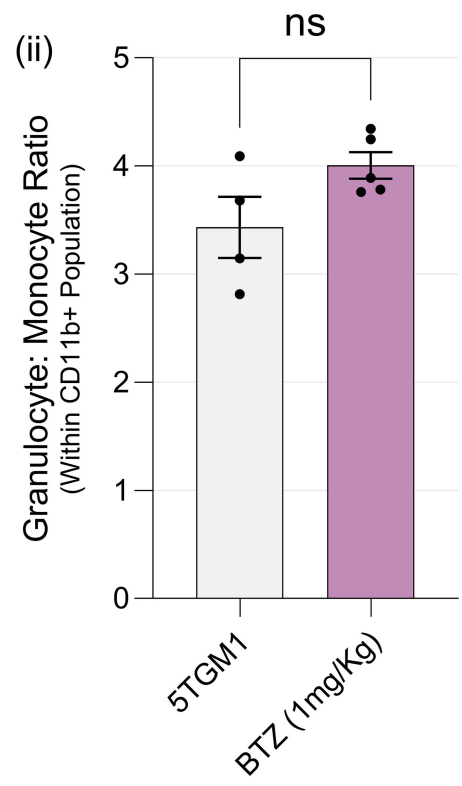
(ii)
ns
Granulocyte: Monocyte Ratio
(Within CD11b+ Population)
5
4
3
2
1
0
5TGM1
BTZ (1mg/Kg)

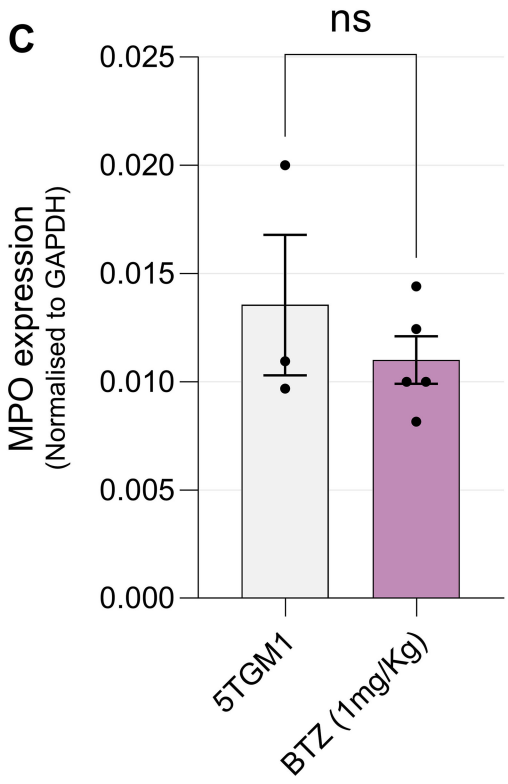
C
ns
MPO expression
(Normalised to GAPDH)
0.025
0.020
0.015
0.010
0.005
0.000
5TGM1
BTZ (1mg/Kg)

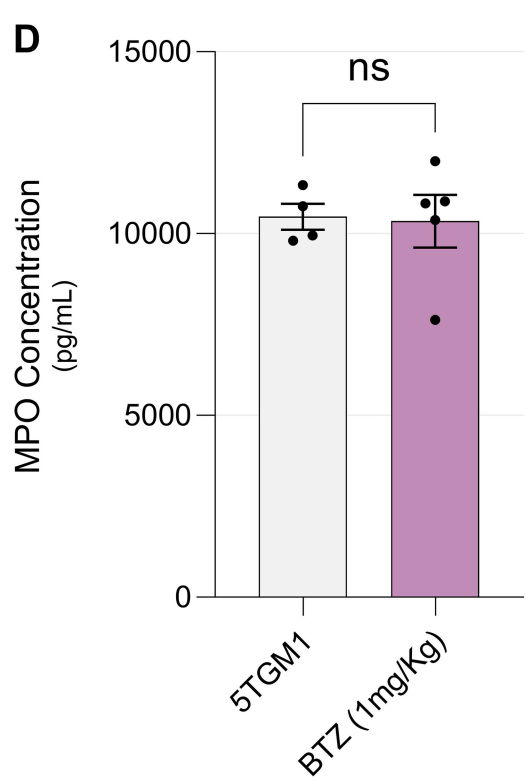
D
ns
MPO Concentration
(pg/mL)
15000
10000
5000
0
5TGM1
BTZ (1mg/Kg)

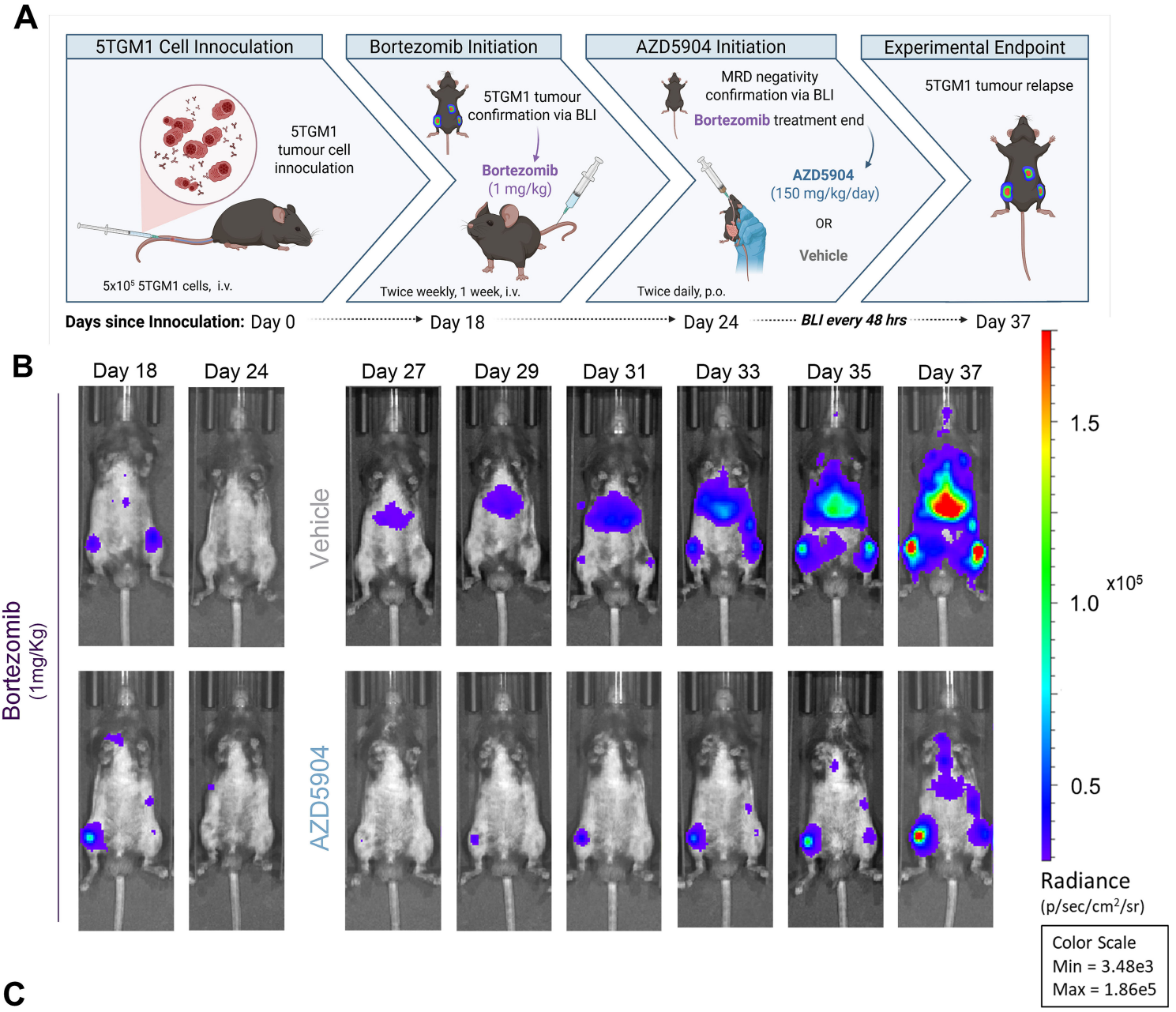
A
5TGM1 Cell Innoculation
Bortezomib Initiation
AZD5904 Initiation
Experimental Endpoint
5TGM1 tumour cell innoculation
5x10⁵ 5TGM1 cells, i.v.
5TGM1 tumour confirmation via BLI
Bortezomib (1 mg/kg)
Twice weekly, 1 week, i.v.
MRD negativity confirmation via BLI
Bortezomib treatment end
AZD5904 (150 mg/kg/day)
OR
Vehicle
Twice daily, p.o.
5TGM1 tumour relapse
Days since Innoculation: Day 0 Day 18 Day 24 BLI every 48 hrs Day 37
B
Day 18
Day 24
Day 27
Day 29
Day 31
Day 33
Day 35
Day 37
Vehicle
AZD5904
Bortezomib (1mg/Kg)
1.5
1.0
0.5
x10⁵
Radiance (p/sec/cm²/sr)
Color Scale
Min = 3.48e3
Max = 1.86e5
C
Total Flux (Photons/ Second)
1.5×10⁷
1×10⁷
5×10⁶
0
Vehicle
AZD5904 (150mg/Kg)
Untreated Tumour Control
Untreated Tumour Control Endpoint
AZD5904 / Vehicle Initiation
(Twice Daily)
BTZ BTZ
**
Day 18
Day 24
Day 27
Day 29
Day 31
Day 33
Day 35
Day 37

Supplementary Methods:

C57BL/KaLwRij CD8+ T cell enrichment and culture

RBC depleted naïve C57BL/KaLwRij splenocytes were enriched using a CD8a$^+$ T Cell Isolation Kit (Miltenyi Biotec), as per manufacturer's instructions. Murine CD8$^+$ T cells were cultured in RPMI-1640 medium with 10% FCS, 0.05 mM β-mercaptoethanol, 1x non-essential amino acids and 2 ng/mL recombinant hIL-2 (R&D Systems).

C57BL/KaLwRij BM-MSC isolation and culture

Primary murine BM-MSCs were isolated by plastic adherence from bone chips of healthy mice. Briefly, long bones (tibiae and femurs) were isolated from 8-week-old C57BL6/KaLwRij and muscle and connective tissue removed using a scalpel blade prior to being cut into small fragments to produce bone chips. Bone chips were transferred into a 75 cm^2 flask and maintained in 20% FCS α-modified minimum essential medium (α-MEM) supplemented with 100 μM ascorbate-2-phosphate, 2 mM L-glutamine, 1 mM sodium pyruvate, 15 mM HEPES, 100 U/mL penicillin, and 100 μg/mL streptomycin. Primary cultures were maintained for 7-10 days, followed by the removal of bone chips from flask and passage of BM-MSCs. BM-MSCs were passaged at least four times before experimental use.

Enzyme-linked immunosorbent assay (ELISA)

Whole blood was collected by cardiac puncture and centrifuged at 2100 x *g* for 10 min to collect serum. Serum was stored at -80°C until required. Commercially available ELISA kits were used to measure levels of MPO (cat. no. DY3667; R&D Systems).

CD11b$^+$ magnetic activated cell sorting (MACS)

Total BM was subject to hypotonic lysis to remove red blood cells (RBC). Samples were centrifuged at 300 x *g* for 10 minutes and supernatant was discarded. Cells were resuspended in magnetic activated cell sorting (MACS) buffer (2 mM EDTA, 0.5% deionized BSA in phosphate-buffered saline) and subjected to negative selection MACS to isolate CD11b$^+$ cells using a CD11b Cell Isolation Kit (Miltenyi Biotec), as per manufacturer's instructions.

Quantitative reverse transcription polymerase chain reaction (RT-qPCR)

Total RNA was extracted using TRIzol (Invitrogen, Waltham, USA) as per manufacturer's instructions. Following RNA isolation, Superscript IV (Invitrogen) was used to synthesize cDNA as per manufacturer's instructions. Quantification of gene expression was achieved using RT^2 SYBR® Green reagent (Qiagen), on a QuantStudio™ 3 Real-Time PCR System (Applied Biosystems, USA)

as previously described [16]. Samples were run in triplicate, and gene expression was analysed using the ΔCt method ($2^{-\Delta Ct}$) normalised to the housekeeping gene *Gapdh*.

Gene	Forward Sequence (5'…3')	Reverse Sequence (5'…3')
Gapdh	TGCACCACCAACTGCTTAG	GGATGCAGGGATGATGTTC
Mpo	TCCCACTCAGCAAGGTCTT	TAAGAGCAGGCAAATCCAG

Supplementary Table 1: Sequences of primers used

Circulating immune cell analysis

At experimental endpoints, blood was collected via terminal cardiac puncture and 50 µL was stored in an EDTA Minicollect tube (Greiner) on ice. Samples were then processed using the Drew Scientific Hemavet 950 Veterinary WBC hematology system (Drew Scientific) for analysis of white blood cells.

Liver toxicity analysis

Serum was collected at experimental endpoint via terminal cardiac puncture as described above. Markers of liver toxicity were assessed in serum (bilirubin, alkaline phosphatase, aspartate aminotransferase and alanine transaminase) by the Roseworthy Veterinary Hospital (RVH) Pathology Laboratory (The University of Adelaide, Roseworthy SA).

In vitro luminol assay

MPO activity *in vitro* was determined by assaying luminol substrate oxidation and luminescence. hMPO (2 µg/mL) was added in triplicate to a 96 well black walled flat bottom plate in 40 µL of 150 mM NaCl solution. AZD5904 was added to corresponding wells at varying concentrations (0.01 µM, 0.1 µM, 1 µM, 10 µM, and 100 µM final) in 40 µL of 150 mM NaCl solution. After 20 minutes, 80 µL of 2 mM luminol sodium salt (Sigma Aldrich) solubilised in 150 mM NaCl was added to each well. Plates were immediately analysed by luminescence using the Xenogen IVIS® Spectrum Imaging System following the addition of 80 µL of 150 µM hydrogen peroxide.

Statistical analysis

Experimental groups were compared using t-test, one way, or two-way analysis of variance (ANOVA) as appropriate. P-values of <0.05 were deemed to be statistically significant. All statistical analyses were conducted using GraphPad Prism (version 9.0, GraphPad Software Inc).

Supplementary Figures:

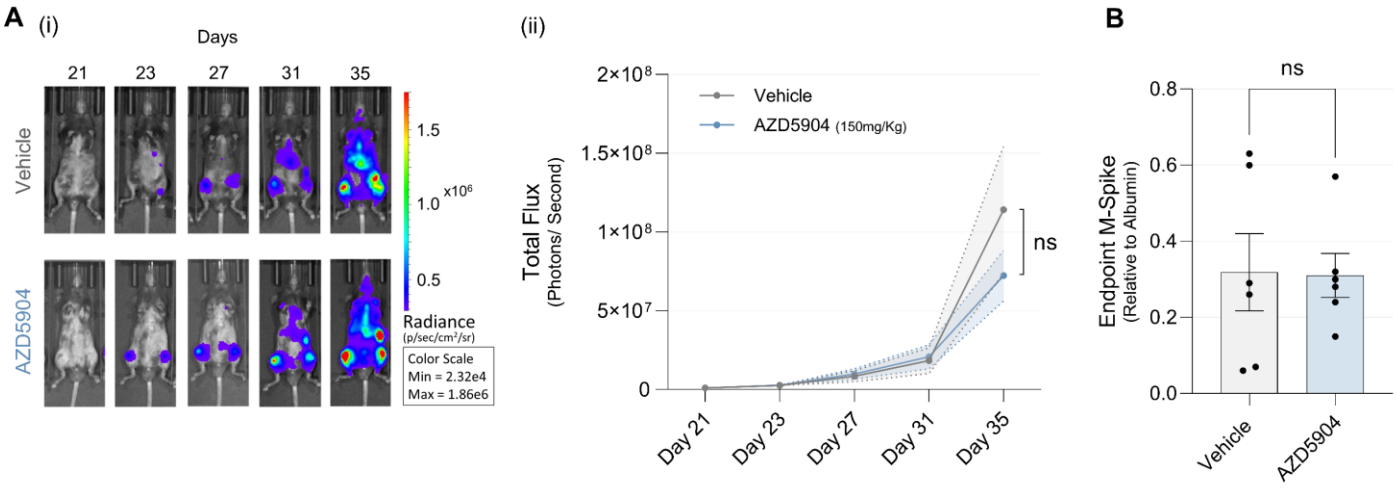

Supplementary Figure 1. AZD5904 treatment initiation at first signs of disease has no effect on tumour progression in C57BL/KaLwRij mice. Six to eight-week-old C57BL/KaLwRij mice were treated with AZD5904 (150 mg/kg; o.g.) twice daily initiated 21 days following 5TGM1 cell inoculation. **A)** (i) Representative ventral BLI images, (ii) ventral tumour progression over time was quantified as photons per second. **B)** Endpoint tumour burden measured by serum protein electrophoresis (SPEP) (day 35) normalised to internal albumin. Results are shown as the mean ± SEM, n=5-6 mice/group. Two-way and one-way ANOVA with Šídák's multiple comparisons test or Tukey's multiple comparisons test, respectively, were used to calculate significance where appropriate, ns (non-significant; $p>0.05$).

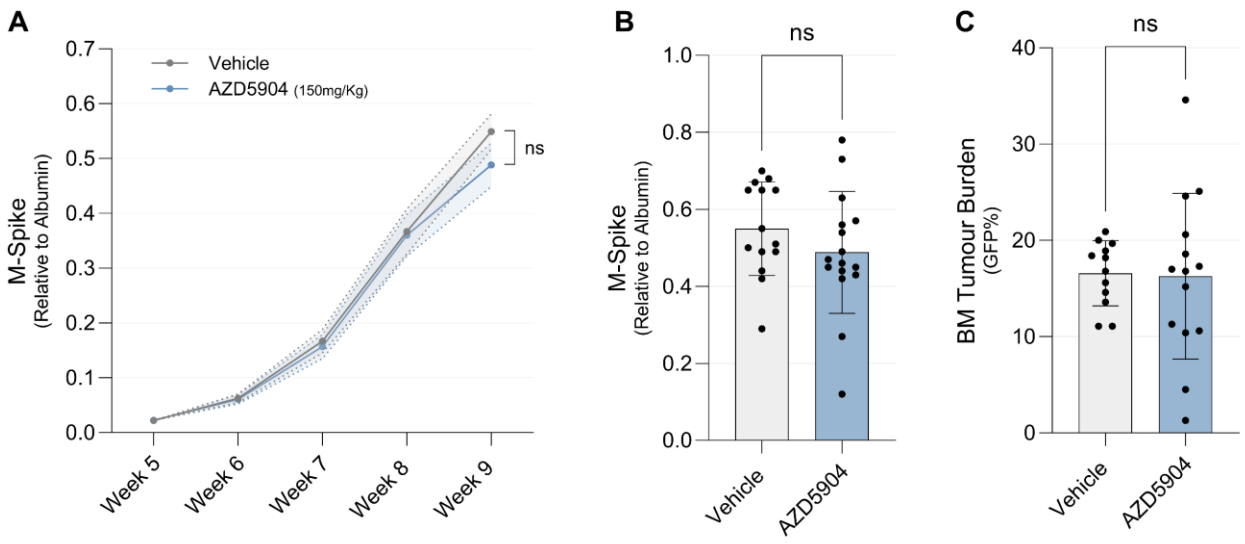

Supplementary Figure 2. AZD5904 treatment initiation at first signs of Vk*Myc tumour by SPEP has no effect on tumour progression in C57BL/6J mice. Eight-week-old C57BL/6J mice were injected with Vk*Myc MM cells (i.v.) and allowed to engraft and establish over 5 weeks. At first signs of disease, as determined by the presence of an M-Spike by SPEP, twice daily treatment with AZD5904 (150 mg/kg; oral gavage) was initiated and continued until experimental endpoint. **A)** Tumour Progression as determined by weekly SPEP **B)** and endpoint SPEP values of individual mice. **C)** Hind limb BM tumour burden as determined by GFP percentage. Results are shown as the mean ± SEM, n=12-16 mice/group. Two-way ANOVA with Šídák's multiple comparisons test **(A)** or unpaired t-test **(B, C)** was used to calculate significance, ns (non-significant; $p>0.05$).

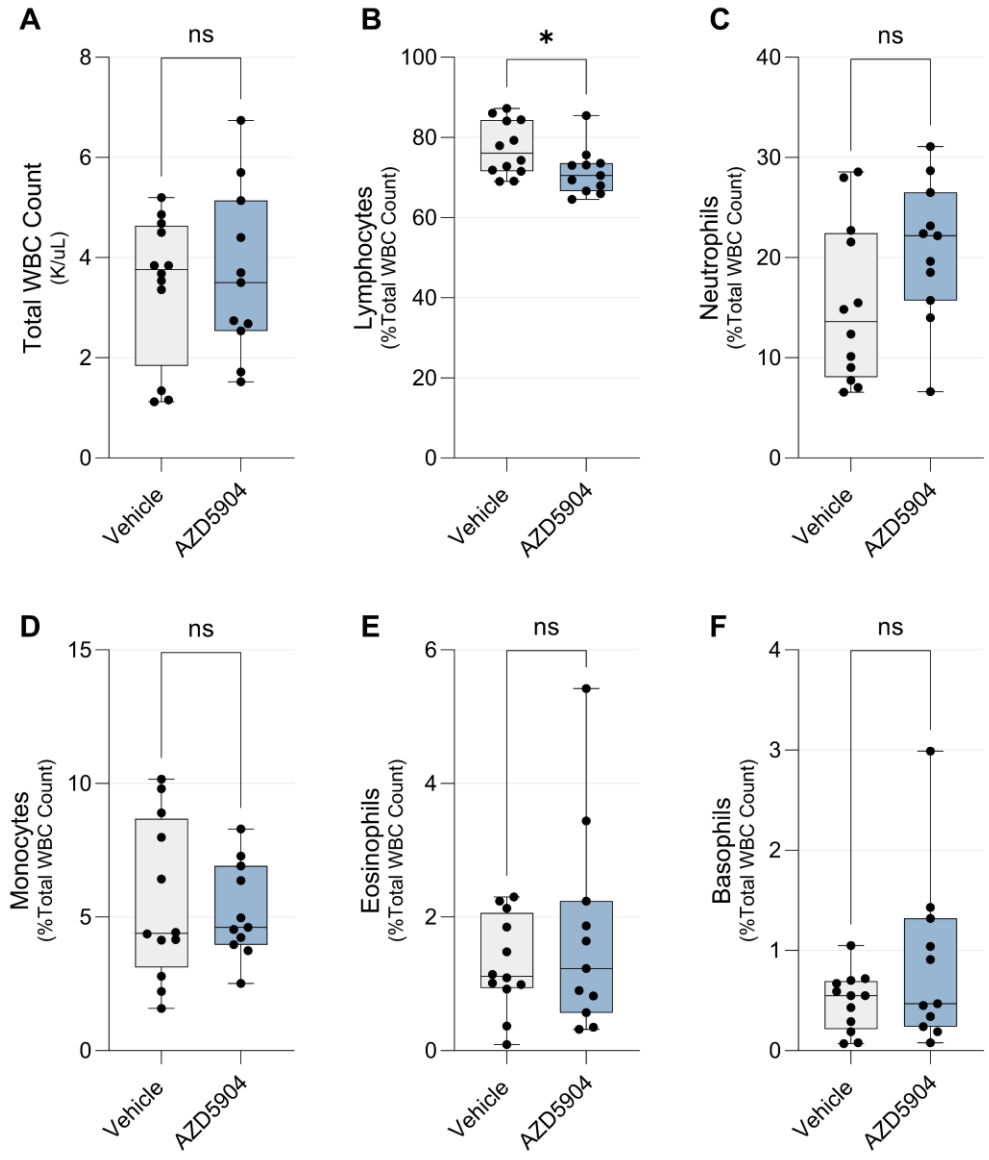

Supplementary Figure 3. Endpoint circulating immune populations in mice receiving AZD5904 treatment at time of Vk*Myc tumour cell inoculation. A) Total white blood cell counts in circulating blood. Percentage of **B)** Lymphocytes **C)** Neutrophils **D)** Monocytes **E)** Eosinophils and **F)** Basophils within total white blood cell count. Box and whisker plots show the median and interquartile ranges (IQRs) between 25% (Q1) and 75% quartiles (Q3), the lower and upper whiskers indicate minimum and maximum values respectively, n=11-12 mice/group. Statistical significance was calculated by unpaired t-test, *p<0.05 and ns (non-significant; p>0.05).

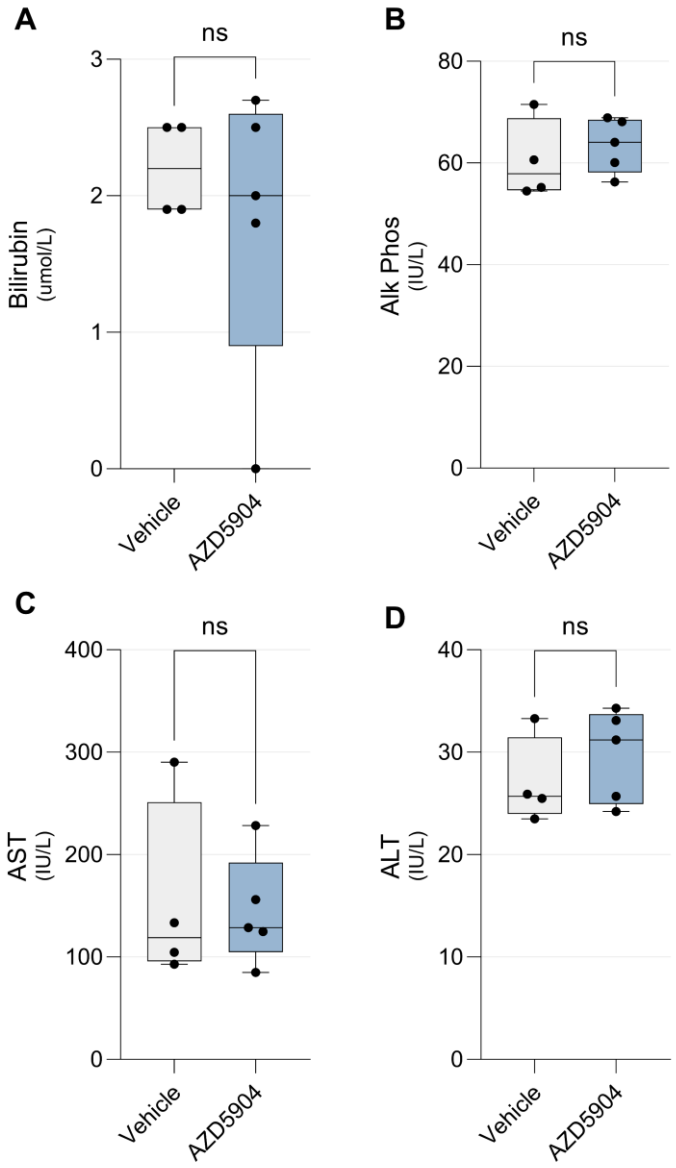

Supplementary Figure 4. AZD5904 does not induce liver toxicity in Vk*Myc tumour bearing mice. Serum was assessed against a panel of markers to assess for liver toxicity, consisting of **A)** bilirubin *(Normal Range: <5.1 µmol/L)* **B)** alkaline phosphatase *(Normal Range: 16-200 IU/L)* **C)** aspartate aminotransferase (AST) *(Normal Range: 46-221 IU/L)* and **D)** alanine transaminase (ALT) *(Normal Range: 22-133 IU/L)*. Box and whisker plots show the median and interquartile ranges (IQRs) between 25% (Q1) and 75% quartiles (Q3), the lower and upper whiskers indicate minimum and maximum values respectively, n=4-5 mice/group. Statistical significance was calculated by one-way ANOVA, ns (non-significant; $p>0.05$).

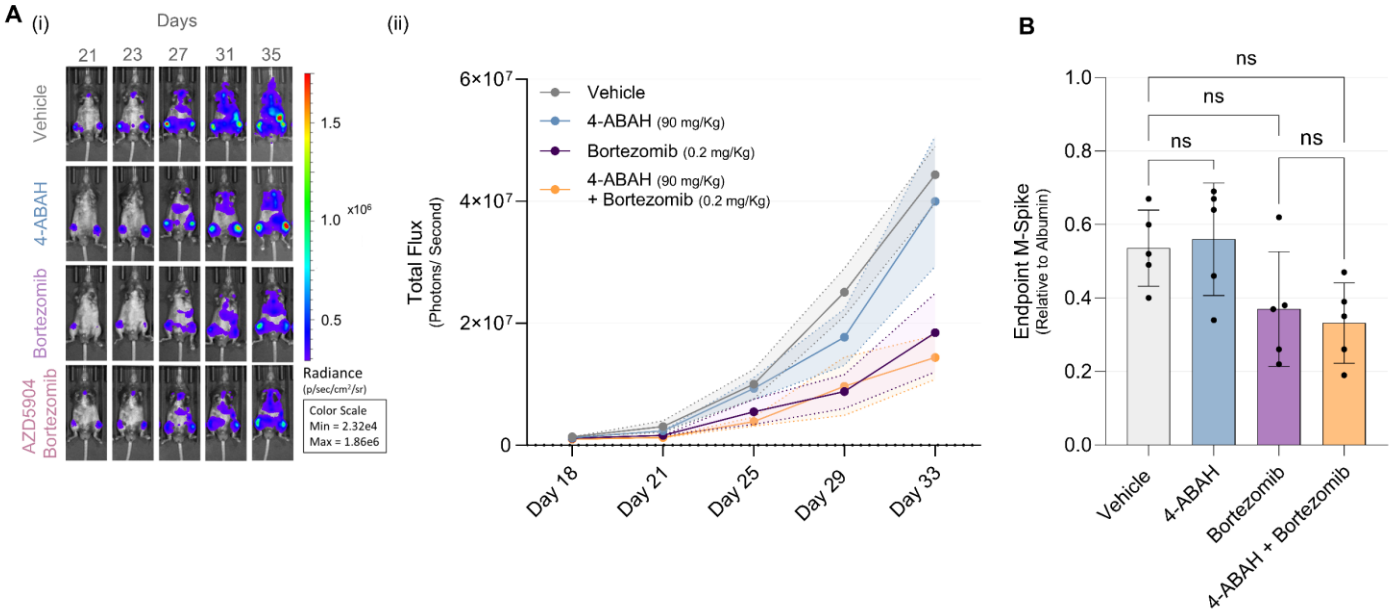

Supplementary Figure 5. 4-ABAH does not potentiate the anti-tumour effects of bortezomib. Six to eight-week-old C57BL/KaLwRij mice were treated with 4-ABAH (40mg/kg; i.p.) twice daily and bortezomib (0.2 mg/kg; i.v.) twice weekly initiated 18 days following 5TGM1 cell inoculation at first sign of disease by BLI. **A)** (i) Representative ventral BLI images. (ii) Ventral tumour burden quantified as photons per second. **B)** Endpoint tumour burden measured by serum protein electrophoresis (SPEP) (day 28) normalised to internal albumin. Results are shown as the mean ± SEM, n=5 mice/group. Two-way and One-way ANOVA with Šídák's multiple comparisons test or Tukey's multiple comparisons test respectively were used to calculate significance where appropriate, ns (non-significant; $p>0.05$).

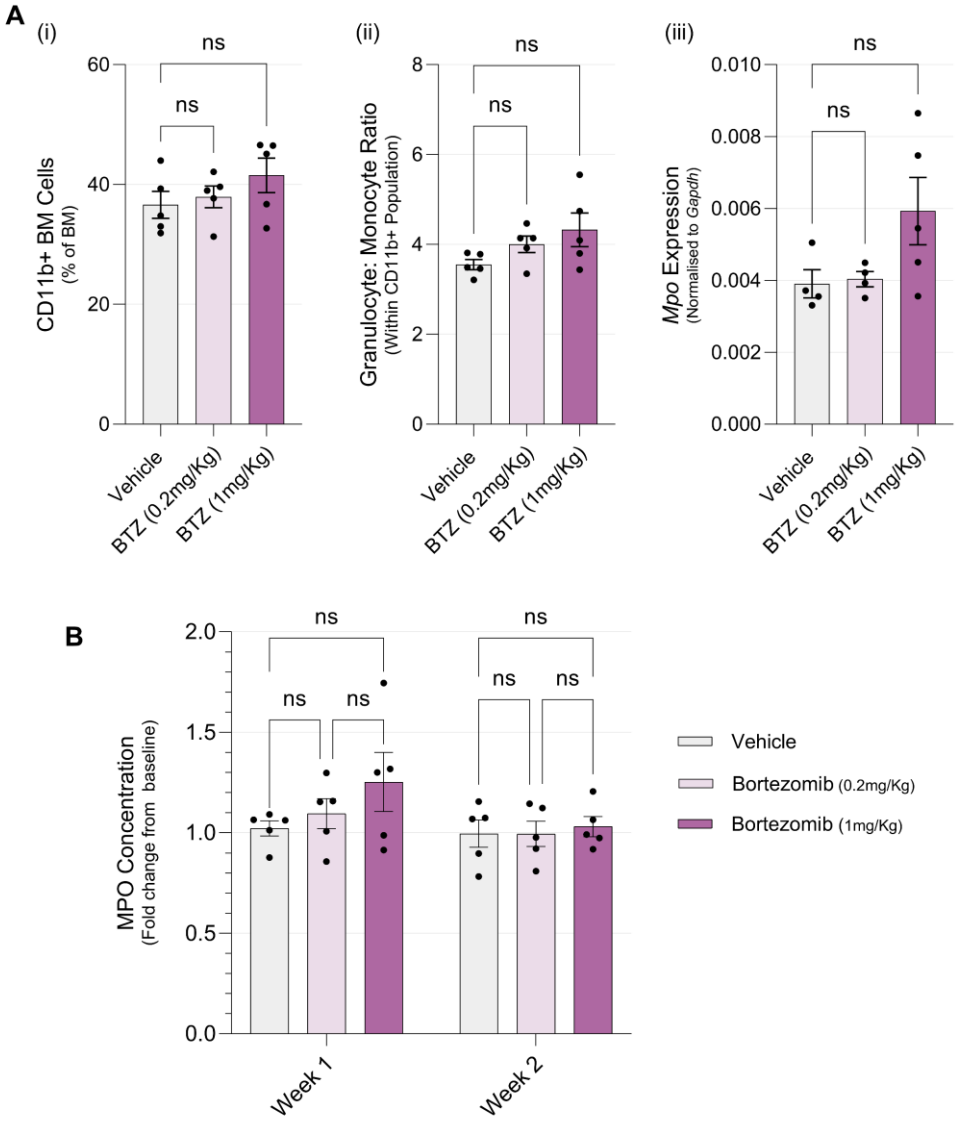

Supplementary Figure 6. Characterisation of myeloid populations in naive C57BL/KaLwRij mice following bortezomib treatment. Eight-week-old tumour naïve C57BL/KaLwRij mice were treated twice weekly with either a subtherapeutic dose (0.2 mg/kg; i.v) or therapeutic dose (1 mg/kg; i.v) of bortezomib twice weekly for two weeks. **A)** (i) The proportion of $CD11b^+$ myeloid cells within the BM after 2 weeks of bortezomib treatment, (ii) The ratio of granulocytes to monocytes within the total $CD11b^+$ myeloid cell population and (iii) Mpo mRNA expression in magnetically activated cell sorting (MACS)-enriched $CD11b^+$ cells. **B)** Change in serum MPO concentration of individual mice over time starting one day prior to bortezomib initiation, after 2 doses of bortezomib (week 1) and after 4 doses of bortezomib at experimental endpoint (week 2). Results are shown as the mean ± SEM, n=5 mice/group. One-way and Two-way ANOVA with Tukey's multiple comparisons test or Šídák's multiple comparisons test respectively were used to calculate significance where appropriate, ns (non-significant; $p>0.05$).